Thesis Report

on

Finite Element Modeling and Analysis of Drive Chain

Submitted in partial fulfilment of the requirement

for the award of degree of

Master of Engineering

In

CAD / CAM & Robotics.

Submitted By

Nanade Sunny H.

801081019

Under the Guidance of

Anirban Bhattacharya,

Assistant Professor,

Department of Mechanical Engineering,

Thapar University, Patiala.

Department of Mechanical Engineering,

Thapar University,

Patiala. – 147004.

July 2012

DECLARATION

I hereby declare that work done in this Thesis Report entitled, **"Finite Element Modelling and Analysis of Drive Chain"** submitted towards partial fulfilment of requirement for award of **Master of Engineering** degree in **CAD/CAM & Robotics** in **Mechanical Engineering Department** of **Thapar University, Patiala,** is an authentic record of work carried out by me under the supervision and guidance of **ANIRBAN BHATTACHARYA, Assistant Professor** of **Mechanical Engineering Department, Thapar University, Patiala.**

This matter embodied in this report has not been submitted in part or full to any other university or institute for the award of any degree.

Nanade Sunny H.

This is to certify that above declaration made by the student concerned is correct to the best of my knowledge & belief.

16/07/2012

ANIRBAN BHATTACHARYA
ASSISTANT PROFESSOR-MED
THAPAR UNIVERSITY, PATIALA

Countersigned by:

DR. AJAY BATISH
PROFESSOR & HEAD-MED
THAPAR UNIVERSITY, PATIALA

DR. S.K. MOHAPATRA
DEAN, ACADEMIC AFFAIRS
THAPAR UNIVERSITY, PATIALA

ACKNOWLEDGEMENT

Words are often less to reveal ones deep regards. With an understanding that work like this can never be the outcome of a single person. I take this opportunity to express my profound sense of gratitude and respect to all those who directly or indirectly helped me through the duration of this work.

I take the opportunity to express my heartfelt adulation and gratitude to my supervisor Mr. Anirban Bhattacharya for his unreserved guidance, constructive suggestions, thought provoking discussions and unabashed inspiration in the nurturing work. It has been a benediction for me to spend many opportune moments under the guidance of the perfectionist at the acme of professionalism. The present work is testimony to his activity, inspiration and ardent personal interest, taken by him during the course of his work in its present form. I am grateful to Dr. Ajay Batish, Professor and Head, Mechanical Engineering Department for providing the facilities for the completion of the work especially regarding simulation and always being a shelter in the odd days.

The work of computation is piecemeal without proper Computational Hardware Support. I would like to wholeheartedly thank Dr. Rajinder Kumar Sharma, Professor & Head, CITM and Mr. Harcharan Jit Singh, Systems Analyst Cum Programmer, CITM for providing me necessary workstations for simulation purpose without which the work would be zero. Necessity being the mother of all inventions, I would like to thank Rockman Industries Ludhiana, who had created the necessity of the work which help me create my basic platform and financially assisting me. Mr. A Shanmugam, Sr. Manager – R&D for assisting me whole heartedly throughout the work. Mr. Sumit Utreja – Vice President for granting such a beautiful work.

I take pride of myself being son of ideal parents and a brother of caring sister for their everlasting desire, sacrifice, affectionate blessings, and help, without which it would not have been possible for me to complete my studies.

No words acknowledge the support I received from my friends for their valorous help and co-operation. I would like to thank all the members and employees of Mechanical Engineering Department, Thapar University, Patiala for their everlasting support. Above all, I express my indebtedness to the "ALMIGHTY" for all his blessings and kindness.

Nanade Sunny H.

801081019.

ABSTRACT

The process of Drive Chain Analysis is as important as its production. In today's era, it's an intelligent and profit making job to produce an optimum product. Currently, testing of chains requires machines on which a specimen is mounted and testing is done. These testing are carried out at hourly, daily or monthly rates depending upon the type of test. Some test machines are limited to a particular dimension of the product. Many changes have to be done in production as well as testing machines if it is thought to change the dimension of product, which needs a huge amount of money, time and manpower. Even if the work is limited to the testing of finished parts, there are many tests which cannot favour dimensional change.

Use of computer software's can help us a lot in the field of optimization. Models for Ultimate Testing, Endurance Testing, and Fatigue Analysis can now days be successfully analysed on a computer. Models whose output agrees with the data form the existing test machines were tried to be made, once done, the chain was optimized based on the constraints.

Table of Contents

LIST OF FIGURES

LIST OF TABLES

Chapter 1 INTRODUCTION

1.1 What is a Chain ?

A chain is a machine component, which transmits power by means of tensile forces, and is used primarily for power transmission. The function and uses of chain are similar to a belt. There are many kinds of chain. Chain can be sorted by either material of composition or by method of construction.

The chains can be sorted into four types as shown below:

1. Cast steel chain
2. Plastic chain
3. Forged chain
4. Steel chain

Classification of Chain according to their use:

1. Power transmission chain
2. Small pitch conveyor chain
3. Free flow chain
4. Large pitch conveyor chain
5. Precision conveyor chain
6. Top chain

The first chain is used for power transmission while the other five chains are used for conveyance.

1.2 Typical Structure of Power Transmission Chain

A typical configuration for 428 type chain is shown in Figure 1.1.

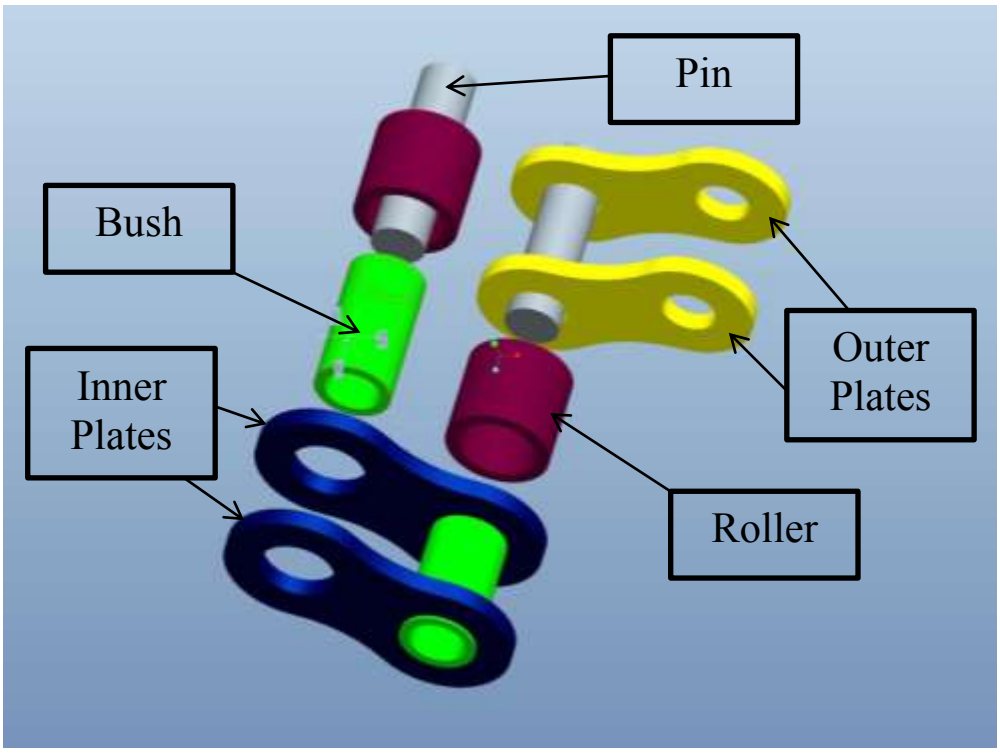

Figure 1.1: The Basic Components of Transmission Chain.

A chain assembly consist of five main components:

1. Inner Plate
2. Outer Plate
3. Roller
4. Bush
5. Pin

While manufacturing the chain, inner plate is press fitted on both the sides of the bush and pin is press fitted on the outer plate. The pin is inserted in between the bush and the bush is inserted in between the roller.

1.3 Functions of Chain Parts

Pin

The pin is subject to shearing and bending forces transmitted by the plate. Along with bush it forms a load-bearing part during chains engagement with sprocket. Hence, the pin

needs high tensile and shear strength, resistance to bending, and also must have sufficient endurance against shock and wear.

Bushing

The bushing is subject to shearing and bending stresses transmitted by the plate and roller, and also gets shock loads when the chain engages the sprocket. When the pin and bush mate, the inner surface forms a load-bearing part together with the pin. The outer surface also forms a load-bearing part with the roller's inner surface when the roller gets engaged with the sprocket. Hence, great tensile strength against shearing is expected and be resistant to dynamic shock and wear.

Roller

Roller is subjected to impact load when it strikes with sprocket teeth during the chain engagement with the sprocket. After completion of the engagement, the roller changes its point of contact and balance. It gets held between the sprocket teeth and bushing, and moves further with the tooth face while receiving a compression load.

Furthermore, the roller's inner surface constitutes a bearing part together with the bushing's outer surface when the roller rotates on the sprocket. Hence, it must be resistant to wear and still have strength against fatigue, compression and shock.

Sprockets

The chain converts rotational power to pulling power, or pulling power to rotational power, by engaging with the sprocket (Figure 1.2). The driver and driven sprockets of the chain drive are of 14 teeth and 44 teeth respectively.

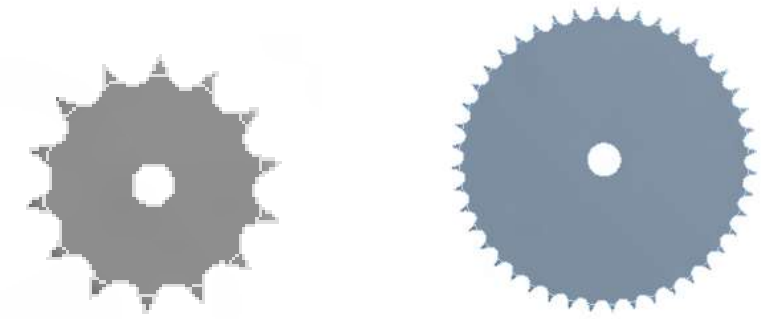

Figure 1.2: Driver and Driven Sprocket.

1.4 Features of Chain Drives

1. Chain can accommodate long shaft with center distances less than 4 m, and is more versatile.
2. Chain can be used with multiple shafts or drives with both sides of the chain.
3. Speed reduction/increase of up to seven to one can be easily accommodated.
4. Standardization of chains under the American National Standards Institute (ANSI), the International Standardization Organization (ISO), and the Japanese Industrial Standards (JIS) allow ease of selection.
5. It is easy to cut and connect chains.
6. The sprocket diameter for a chain system may be smaller than a belt pulley, while transmitting the same torque.
7. Sprockets are subject to less wear than gears because sprockets distribute the loading over their many teeth.

1.5 Testing of Drive Chain

Companies manufacturing chain drive usually do the testing of the drive chain in order to see whether the manufactured chain is upto their requirements. Also to survive in the competitive market the testing of chain allows the manufacturers to see what strength does their chain have and how superior or inferior their chain is as compared to the other manufacturers. A chain manufacturing company in Ludhiana does the following test before the dispatch of the chain in order to confirm its quality:

1. Tensile Test
2. Fatigue Test
3. Endurance Test

1.5.1 Tensile Test

A chain can transmit tension, but usually cannot transmit pushing forces. Only a few special chains are available that can push, but this discussion focuses on tension.

How will the chain behave when it is subject to tensile loading? There is a standard test to determine the tensile strength of a chain. Here's how it works: The manufacturer takes a new, three-link-or-longer power transmission chain and firmly affixes both ends to the jigs (Figure 1.3). Now a load or tension is applied and measurements are taken until the chain breaks (IIS B 1801-1990)

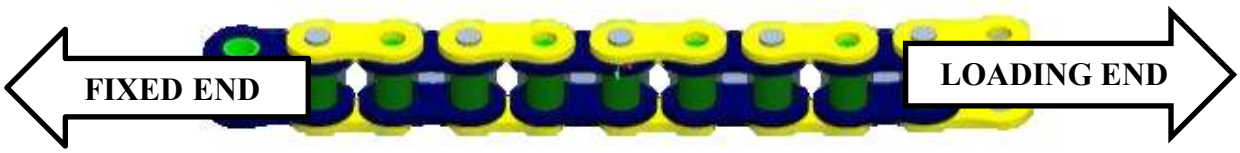

The load at which the chain breaks is the ultimate tensile strength of the chain. Figure 1.4 shows the tensile test apparatus and its value for a particular test.

Figure 1.4: Tensile Strength of Chain.

1.5.2 Fatigue Test

Fatigue tests consist of testing the chain for a repetitive load. The number of cycles the chain can withstand is the fatigue life of the chain. Figure 1.5 shows the testing arrangement for fatigue test. One end of the chain is fixed and load is applied on the other end. This load increases gradually. Apart from the tensile test in which the load was increased till the chain breaks, there is a certain limit to the applied load in fatigue test. The load starts from a minimum load of 38 kgf and gradually increased to 420 kgf. Once this maximum load is reached, the load is gradually decreased again to 38 kgf. The number of cycles a particular chain can withstand is noted as the fatigue life of the chain.

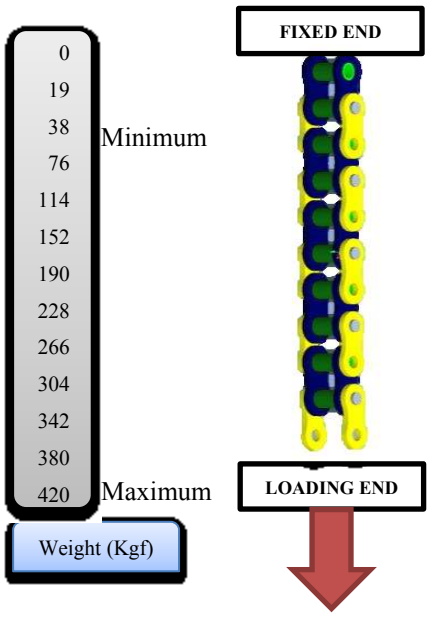

Figure 1.5: Fatigue Testing of Drive Chain

The loading condition is different for different types of chain. For the current chain under consideration, expected fatigue life is 1e7 cycles.

1.5.3 Endurance Test

Endurance testing is done to see the effect of actual loading on the chain drive. Figure 1.6 shows the arrangement for endurance testing. A motor is attached with the drive sprocket which drives it at 2000 rpm. A load of 5 KW is connected on the driven sprocket.

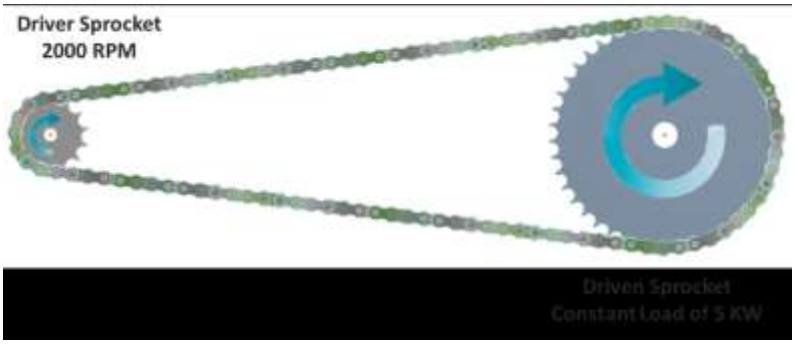

Figure 1.6: Endurance Testing of Chain Drive.

This test rig is run for 100 hours. The elongation of chain is noted at a convenient interval. Figure 1.7 shows the elongation of a chain after the endurance test.

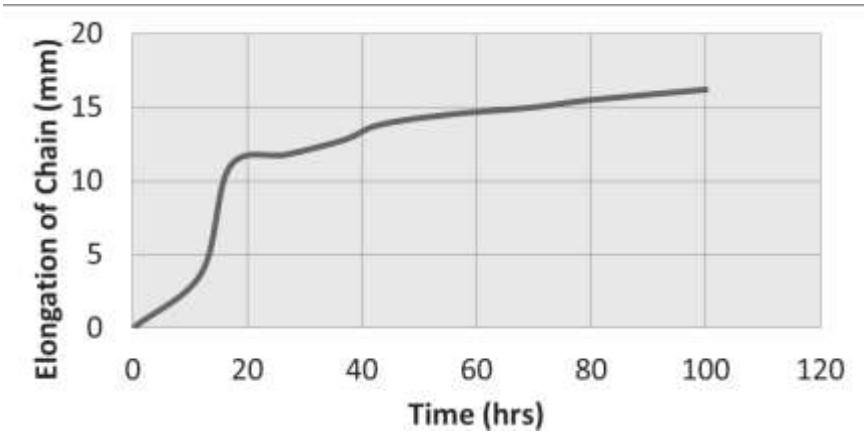

Figure 1.7: Elongation of Chain During Endurance Test.

1.6 Finite Element Method and Analysis

To tackle the many types of problem which are solved in computational physics it will not be surprising that several different kinds of method are available. Here the most common methods in a general way and indicate the kinds of problem that they can solve were described. This general background is intended to do no more than convey the essence of the variety of techniques available to the computational physicist and the range of problem's to which they can be applied. Some of the methods to solve a problem are entailed below:-

1.6.1 The Monte Carlo method

1.6.2 Particle methods

1.6.3 Continuum physics — the finite-difference method

1.6.4 Continuum physics — the finite-element method

The finite-element method can be an alternative to finite-difference methods in some applications, but there are types of problem for which it is most suitable and for which finite-difference methods would be difficult to apply. Where it comes into its own is in linear steady-state problems in two or three dimensions involving configurations with little symmetry and complex boundaries and where there is some global relation which the system must satisfy, such as minimum energy. The region of the problem is defined by a set of points, called nodes, connections between which define elements, shapes in one, two or three dimensions which together either exactly or approximately define the region of interest including the boundary. An example of a set of nodes and elements defining a two-dimensional irregular region is shown in Figure 1.8. The objective of the finite-element method is to find the values of the quantity of interest, say 0, at the nodal points in an equilibrium situation.

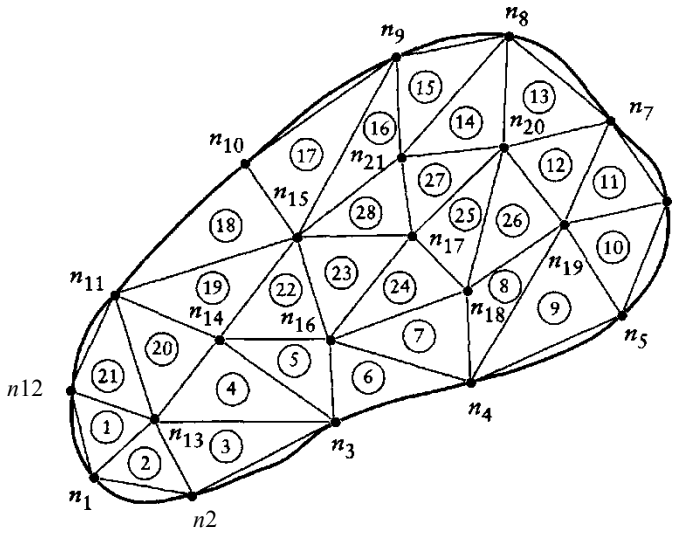

Figure 1.8: A complex shape represented by 21 nodes and 28 triangular elements [1].

Finite element analysis (FEA) has become commonplace in recent years, and is now the basis of a multibillion dollar per year industry. Numerical solutions to even very complicated stress problems can now be obtained routinely using FEA, and the method is so important that even introductory treatments of Mechanics of Materials – such as these modules – should outline its principal features.

In spite of the great power of FEA, the disadvantages of computer solutions must be kept in mind when using this and similar methods: they do not necessarily reveal how the stresses are influenced by important problem variables such as materials properties and geometrical features, and errors in input data can produce wildly incorrect results that may be overlooked by the

analyst. Perhaps the most important function of theoretical modeling is that of sharpening the designer's intuition; users of finite element codes should plan their strategy toward this end, supplementing the computer simulation with as much closed-form and experimental analysis as possible.

Finite element codes are less complicated than many of the word processing and spreadsheet packages found on modern microcomputers. Nevertheless, they are complex enough that most users do not find it effective to program their own code. A number of prewritten commercial codes are available, representing a broad price range and compatible with machines from microcomputers to supercomputers. However, users with specialized needs should not necessarily shy away from code development, and may find the code sources available in such texts as that by Zienkiewicz [2] to be a useful starting point. Most finite element software is written in FORTRAN, but some newer codes such as felt are in C or other more modern programming languages.

In practice, a finite element analysis usually consists of three principal steps:

a. **Preprocessing:** The user constructs a model of the part to be analyzed in which the geometry is divided into a number of discrete sub regions, or "elements," connected at discrete points called "nodes." Certain of these nodes will have fixed displacements, and others will have prescribed loads. These models can be extremely time consuming to prepare, and commercial codes vie with one another to have the most user-friendly graphical "pre-processor" to assist in this rather tedious chore. Some of these preprocessors can overlay a mesh on a preexisting CAD file, so that finite element analysis can be done conveniently as part of the computerized drafting-and-design process.

b. **Analysis:** The dataset prepared by the preprocessor is used as input to the finite element code itself, which constructs and solves a system of linear or nonlinear algebraic equations

$$K_{ij}u_j = f_i$$

where u and f are the displacements and externally applied forces at the nodal points. The formation of the K matrix is dependent on the type of problem being attacked, and this module will outline the approach for truss and linear elastic stress analyses. Commercial codes may have very large element libraries, with elements appropriate to a wide range of problem types. One of FEA's principal advantages is that many problem types can be

addressed with the same code, merely by specifying the appropriate element types from the library.

c. **Postprocessing:** In the earlier days of finite element analysis, the user would pore through reams of numbers generated by the code, listing displacements and stresses at discrete positions within the model. It is easy to miss important trends and hot spots this way, and modern codes use graphical displays to assist in visualizing the results. Typical postprocessor display overlays colored contours representing stress levels on the model, showing a full-field picture similar to that of photo elastic or more experimental results.

1.7 Why is FEA needed?

- To reduce the amount of prototype testing
  - Computer simulation allows multiple "what-if" scenarios to be tested quickly and effectively.
- To simulate designs that are not suitable for prototype testing
  - Example: Surgical implants, such as an artificial knee
- The bottom line:
  - Cost savings
  - Time savings… reduce time to market!
  - Create more reliable, better quality designs

1.8 Applications of FEA

Several modern FEA packages include specific components such as thermal, electromagnetic, fluid, and structural working environments. In a structural simulation, FEA helps tremendously in producing stiffness and strength visualizations and also in minimizing weight, materials, and costs. A variety of specializations under the umbrella of the mechanical engineering discipline (such as aeronautical, biomechanical, and automotive industries) commonly use integrated FEA in design and development of their products.

FEA software provides a wide range of simulation options for controlling the complexity of both modeling and analysis of a system. FEA allows detailed visualization of where structures bend or twist, and indicates the distribution of stresses and displacements. Similarly, the desired level of accuracy required and associated computational time requirements can be managed simultaneously to address most engineering applications. FEA allows entire designs to be constructed, refined, and optimized before the design is manufactured.

This powerful design tool has significantly improved both the standard of engineering designs and the methodology of the design process in many industrial applications. The introduction of FEA has substantially decreased the time to take products from concept to the production line. It is primarily through improved initial prototype designs using FEA that testing and development have been accelerated. In summary, benefits of FEA include increased accuracy, enhanced design and better insight into critical design parameters, virtual prototyping, fewer hardware prototypes, a faster and less expensive design cycle, increased productivity, and increased revenue.

2.1 A Brief History of Chain

The word meaning "chain" can be traced back to an ancient word in the Indo-European language family. As early as 225 BC, chain was used to draw a bucket of water up from a well. This very early bucket chain was composed of connected metal rings.

In the 16th century, Leonardo da Vinci made sketches of what appears to be the first steel chain. These chains were probably designed to transmit pulling, not wrapping, power because they consist only of plates and pins and have metal fittings. However, da Vinci's sketch does show a roller bearing (shown in Figure 2.1).

It took some time for the technology to catch up with the concept. Problems in the manufacturing and processing of steel prevented the chain growth until the 19th century, when new technologies made steel chain and bearings realities. In the 1800s, a Frenchman named Gull obtained a patent for a similar chain for use on a bicycle. This chain, called "Gull Chain," is still used today in hanging applications.

When molded chain was invented in the 19th century, things began to move rather quickly. First came the cast detachable chain, which is composed of identical cast links. Next, the pintle chain, which has a separate pin, appeared. The cast detachable chain and the pintle chain have been improved over the years, and they are still in use today in some special applications. They are being replaced—gradually—by large pitch steel conveyor chain.

In the late 1800s, a new development—the bushing—revolutionized steel chain. Chains with bushings had greater wear resistance than Gull Chain because the bushing acted as a bearing, protecting the pin. At this point, the chain story moves into superspeed. Steel bushing chain was used on bicycles, in the rear-wheel drive of early automobiles, and, in 1903, as the propeller drive in the Wright brothers' airplane.

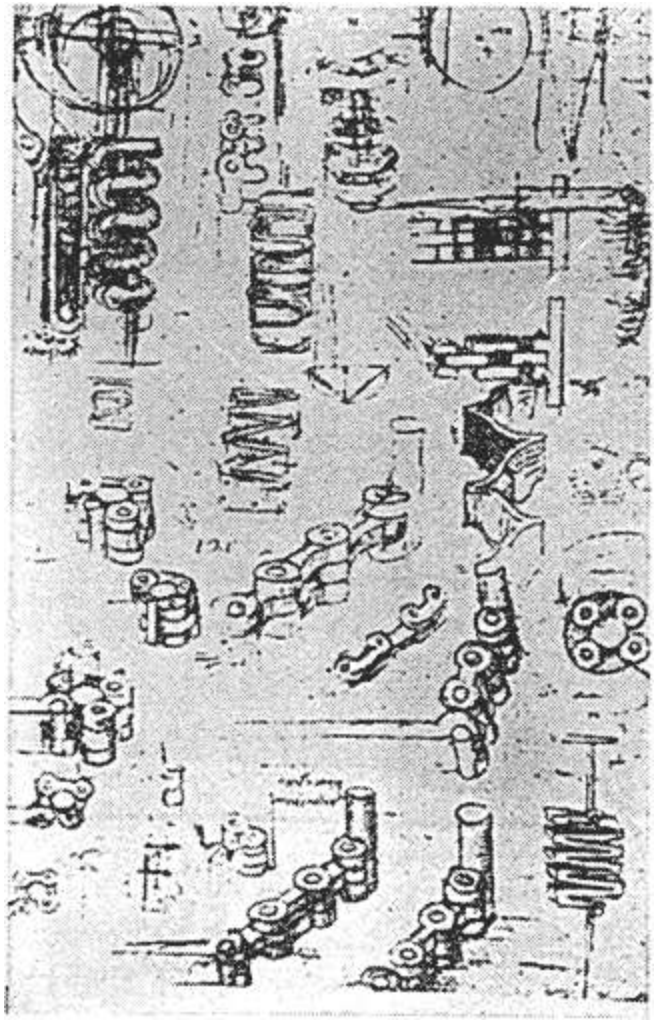

Figure 2.1: First drawing of chain during the Renaissance by Leonardo da Vinci [3].

Chain drive became of interest to the automobile industry with the rise in importance of *noise, vibration and harshness* (NVH). Chain drives offer non-slip, light weight, inexpensive, compact power transmission compared to belt or gears, but usually at the cost of increased noise and vibration. A brief history of chain drives and the important milestones in their practical development through the late twentieth century can be found in Conwell [4].

2.2 Review of literature

Today, three types of chains are commonly found: roller chain, silent chains and engineering steel chains. The work is related to roller chain so further discussion will be limited to chain of this type. Chain drives were poorly understood through the 1980's for a variety of reasons, including the polygonal action, nontrivial sprocket geometry, intentional clearances and

unintentional dimensional variations due to manufacturing tolerances, friction, and the large number of bodies that make up the typical chain and sprocket system [4].

The manufacturer of roller chains has been standardized by the American National Standards Institute under standard B29.1 (ANSI,1972) since 1913. The first report in an ASME journal devoted to the study of roller chain drive based upon sprocket impact loads and experience. Bremer reported on marine applications and analyzed the various loads on chain drives [4].

Binder, Covert presented some analytical relations which may help in developing a better understanding of the mechanics of roller-sprocket impact. Various relative impact velocities were derived. These velocities may be used in impact energy relations for determining limiting sprocket speeds on the basis of roller breakage, noise, heating, and sprocket wear. Some experimental data on roller breakage were presented and used to illustrate a method of organizing data. Impact energy using a certain velocity correlates to some extent with roller breakage. [5]

Staments considered the fundamental loads on chain drives using an optical strain gage. [6]

Most modern work can be directly traced to Binder's classical text. In his work, Binder both documented and extended the work of many early chain investigators. [7]

Polygonal action has been one of the most studied chain drive topics. Morrison [8], Mahalingham [9], Okoshi and Uehara [10] and Bouillon and Tordion [11] all reported on this phenomenon.

Ryabov [12] and Chew [13] modeled the inertia effects on impact forces in chain drives, while Radzimovsky [14]developed an 'equalizing' linkage in an attempt to minimize the impact. Turnbull and Fawcett [15] completed an approximate kinematic analysis of roller chain drives.

Recent research on chain drives has been conducted at the University of Michigan (Johnson), Pennsylvania State University (Wang), University of Texas (Marshek), Chalmers University of Technology (Gerbert) and Columbia University (Freudenstein). Marshek and his students ([16] [17] [18] [19]) determined quasi-static chain and sprocket load distributions.

Eldiwany, Marshek [20] conducted an experimental study to measure the load distribution in steel roller chains on steel sprockets and determine the effect of lubrication, misalignment, sprocket speed of rotation at low speeds, and slack-side load. A chain load distribution test machine was designed and constructed to conduct this investigation. Theoretical results obtained from a geometric progression load distribution model were compared to the experimental results.

Chen and Freudenstein [21]completed an approximate kinematic analysis of the roller chain drive.

Eldiwany, Marshek [20] conducted an experimental study to measure the load distribution in steel roller chains on polymer sprockets and determine the effect of material modulus of elasticity, tight-side load, slack-side load and pitch difference. A chain load distribution test machine and a single sprocket tooth test machine were designed and constructed to conduct this investigation. Theoretical results obtained from a geometric progression load distribution model and a spring model load distribution analysis was compared to the experimental results.

Veikos and Freudenstein ([22] and [23]) developed a lumped mass dynamic model based on Lagrange's equation and also studied chain drive vibrations. Wang's work is based on a continuous model of the axially moving material and he has studied the stability of chain span subject to periodic sprocket excitations [24] and the effect of impact intensity on chain drive vibration [25]. Gerbert studied the tooth load distribution of seated and unseated roller chains and timing belts and made several important observations about the effects of friction and elasticity. Kim and Johnson ([26] and [27]) developed a details model of the roller-sprocket contact mechanics that allowed the first determination of actual pressure angles and a multi-body dynamic simulation based on Kane's dynamic equation. Choi and Johnson ([28] and [29]) incorporated the effects of impact, polygonal action, and chain tensioners into the axially moving material model and studied transverse vibration of chain spans.

The kinematic analysis of combined roller-chain and planar mechanisms was studied [30]. In this paper a mechanical system comprising of two sprocket roller-chains (flexible system) in combination with rigid planar links either crank-coupler or drag-link linkage was suggested. The paper discusses and analyzes two alternatives in which the roller-chain is driving the rigid links and "inverse" possibility when the crank of the rigid planar links is the input element and the output motion was taken from the roller-chain. Moreover, replacing the crank of the rigid links by a variable length was discussed, and obtained by considering the coupler as being joined with a point on a drag-link mechanism. The merits of each version were presented and discussed. Of interest, was the unique advantage of obtaining particular output/input velocity ratios which no available mechanism could achieve. Moreover, the obtained results indicated quite a useful applicability of the analyzed system in the industrial packing process, motion transmission and, in particular, in conveying machinery. The kinematic analysis procedure was presented in simple formulation using trigonometric relations.

The development of a complete model for the dynamic analysis of an automotive timing chain system was performed [31]. In order to produce the most accurate results, all of the system components were modeled, including the rolling and silent chains, the chain guide, the chain arm, the sprockets, and the hydraulic tensioner. The completed model had been used to analyze many different characteristics concerning automotive timing chain systems. The nonlinear model was used to simulate the longitudinal and transverse responses of the timing chain, as well as the chain impact dynamics. A detailed model of the hydraulic tensioner was derived and used to predict the plunger and check ball motions. In addition, both the free and forced vibrations of the model were investigated. For the free vibration analyses, the natural frequencies of the system and the associated mode shapes were analyzed. For the forced vibration analyses, the crank motion and the cam torques were prescribed for the model, and then the vibrational amplitudes for each component were examined. For the production engine considered, the experimental measurements of the plunger motion and the natural frequencies were in good agreement with the analytical results.

A computer-aided analysis for the selection of roller chain drives, which are commonly used in mechanical power transmission systems, was studied [32]. Computer programs were written and proposed to improve the traditional method of drive selection for the roller chain drives. The algorithms were mainly based on the existing equations for the mechanics of the drives, including the geometry and the power transmission capabilities. The purpose of attempting to computerize the selection procedures was to reduce the number of tables and charts that were required in traditional selection routines. In addition, it was also intended to cut down the amount of iteration and calculation work performed. To evaluate the accuracy and limitations of the proposed programs, comparisons were made with the existing examples of drive selections. It was found that the programs implemented in the present selection process were able to substitute for most of the traditional selection charts and tables. Furthermore, the selection using the proposed methodology could be performed in a shorter time owing to the computer-generated process.

Construction and instrumentation of a machine to measure tension and impact forces in roller chain drives [33]. The design and construction of a new test machine configuration that offers some advantages over the traditional design was discussed. The new machine and attendant instrumentation provided more realistic chain loading, and allowed link tension and roller-sprocket impact monitoring during normal operation. The incorporation of an idler sprocket

allows independent adjustment of test span length and preload. The angle at which rollers approach an instrumented sprocket could also be adjusted. Drawbacks of the new configuration (compared to the four-square design) were that the support structure may not be as rigid and the additional sprockets (idler sprocket and instrumented sprocket) added kinematic complexity.

A strain gage mounted on a link side plate was used to determine chain tension during normal operation over a wide range of linear chain speeds and preloads [34]. The test machine also included specially instrumented idler sprocket that allowed the measurement of the horizontal and vertical components of the bearing reaction force. The roller-sprocket impact force was then computed by an experimental transfer function approach facilitated by a Bruel & Kjaer 2032 dual channel spectrum analyzer.

A practical approach for predicting the meshing noise due to the impact of chain rollers against the sprocket of chain drives was presented [35]. An acoustical model relating dynamic response of rollers and its induced sound pressure was developed based on the fact that the acoustic field was mainly created by oscillating rigid cylindrical rollers. Finite element techniques and numerical software codes were employed to model and simulate the acceleration response of each chain roller which was necessary for noise level prediction of a chain drive under varying operation conditions and different sprocket configurations. The predicted acoustic pressure levels of meshing noise were compared with the available experimental measurements. It was shown that the predictions were in reasonable agreement with the experiments and the approach enabled designers to obtain required information on the noise level of a selected chain drive in a time- and cost-efficient manner.

Kinetostatic analysis of a roller drive was performed [36]. It was found that the roller drive has a speed fluctuation that corresponds with the number of ring gear rollers, and the magnitudes of the forces vary periodically with the crank angular displacement; hence, the roller drive has an input torque ripple. It was also found that the roller drive has high efficiency under the operation of high speed. The kinematic modeling on the basis of vector loop approach was developed, and models for analyzing the kinetostatics and mechanical efficiency of roller drives considering friction were proposed. For a given a roller drive, the loads acting on the conjugated joints, such as the planet gear and crank, the planet gear and ring gear roller, and the planet gear and disc plate, can be investigated by using the models. The results showed that the roller drive has a speed fluctuation that corresponds to the number of ring gear rollers, and the magnitudes of the

forces vary periodically with the crank angular displacement. It was also found that the roller drive has an input torque ripple caused by the forces acting on the conjugated joints with periodic variation and fluctuation in the output speed. In addition, the influence of the geometric parameters on efficiency and speed fluctuation of the roller drives were discussed. It was also shown that the speed fluctuation of the roller drives can be decreased by reducing the radius of the ring gear and the crank eccentricity, and by increasing the radius of the planet gear, the radius of the ring gear roller and planet gear roller.

Investigation to study the optimization of the chain drive system on sports motorcycles [37]. They created a new model to predict the efficiency of a 600cc sports motorcycle at different speeds. The transmission efficiency is estimated to be between 96 and 99% for speeds less than 75 mile/h. Between 75 and 150 mile/h the transmission efficiency can be as low as 85% due to inertial tension. The transmission efficiency model presented in this paper enables optimization of sprocket and chain sizes. In general, large sprockets are better at low speeds and smaller sprockets are better at high speeds. The optimum chain size is the chain with the smallest pitch that can meet the torque and power requirement. The sprocket center distance also had a big effect on efficiency and it is important to use an effective installation procedure. In particular, it is important to set a chain up when the rear wheel axle, front crank and swing arm bearing are all in-line.

A model of a roller chain drive was developed and applied to the simulation and analysis of roller chain drives of large marine diesel engines [38]. The model included the impact with guide-bars that were the motion delimiter components on the chain strands between the sprockets. The main components of the roller chain drive model include the sprockets with different sizes and the chain made of rollers and links, which were represented by rigid bodies, mass particles and springs–damper assemblies respectively. The guide-bars were modeled as rigid bodies with a roller-guide contact representation as continuous force. The model of the roller-chain drive then proposed departed from an earlier model where two contact/impact methods were proposed to describe the contact between the rollers of the chain and the teeth of the sprockets. These different formulations were based on unilateral constraints and continuous force methods, respectively.

In the unilateral constraint methodology the kinematic constraints were introduced in the system anytime a contact between the rollers and the sprockets was detected. The condition for the constraint addition was based on the relative distance between the roller center and the sprocket

center, i.e. a constraint was added when such distance is less than the pitch radius. The unilateral kinematic constraint was removed when its associated constraint reaction force, applied on the roller, is in the direction of the root of the sprocket teeth. In order to improve the numerical efficiency of the methodology only the first and last roller seated on each sprocket and the two free rollers nearest to the sprocket were checked for capture or release. It was assumed that all the rollers in the chain, between the first and last seated rollers were in contact with the sprocket.

In the continuous force method the roller-sprocket contact, was represented by forces applied on each seated roller and in the respective sprocket teeth. These forces were functions of the pseudo penetrations between roller and sprocket, impacting velocities and a restitution coefficient. In the continuous force method, an arc of circle approximates the geometry of the tooth profile. In both models it was assumed that all the rollers of a chain strand are not in contact with any particular sprocket. The contact between the rollers of the chain strands and the guide-bars was modeled with the continuous force model. The methodology was implemented in a computational code to study the dynamics of the drive, including the chain flexibility, transversal and longitudinal vibrations and contact forces between the chain and sprockets. The models proposed effectively represented the polygonal effect, always present in this type of drives, and therefore, all vibration dynamics associated to it. The inclusion of the guide-bars allows the usage of the chain drive model in situations relevant for implementation of the real diesel engines in large maritime vessels.

A model of a roller-chain drive was developed and applied to the simulation and analysis of roller-chain drives of large marine diesel engines [39]. Two different ways of modeling the contact between the rollers and sprockets were presented; one using a circular shaped tooth profile and the other using the shape of a real tooth profile. The main components of the roller-chain drive model included the sprockets with different sizes and the chain made of rollers and links, which were represented by rigid bodies, mass particles and spring-damper assemblies, respectively. The contact between the rollers and the sprockets were represented by a continuous contact force. The models proposed effectively represent the polygonal effect always present in this type of drive. The numerical results from the simulations were compared with analytical results, for simplified models. The model with a real tooth profile proves superior to the model with a circular tooth profile.

Bush chains and roller chains are frequently used in valve train systems of combustion engines [40]. Their complex dynamical behavior was dominated by the effects of high velocities and transient driving torques as well as by polygonal action and rotatory impacts.

These phenomena may be studied efficiently by the methods of multibody dynamics. However, the high-frequency characteristics and the comparatively large number of degrees of freedom caused challenging numerical problems. There are two basic strategies to keep the numerical effort in time integration within reasonable bounds: On the one hand it may be reduced by adapted modeling, on the other hand specific time integration schemes may be used to solve the equations of motion. The paper introduces methods in both fields and presents simulation examples to show their effect on efficiency and to validate their implementation.

Investigation of the wear of roller drive chains showed that the spacing in the external chain elements limits the operational fitness of the transmission. Improved criteria of transmission performance in terms of chain coupling were recommended. [41]

The coupling in a chain transmission was investigated. Parametric optimization of the sprocket design was considered. [42]

The modal characteristics of the transverse vibration of an axially moving roller chain coupled with lumped mass were analyzed [43]. The chain system was modeled by using the multi-body dynamics theory and the governing equations were derived by means of Lagrange's equations. The effects of the parameters, such as the axially moving velocity of the chain, the tension force, the weight of lumped mass and its time-variable assign position in chain span, on the modal characteristics of transverse vibration for roller chain were investigated. The numerical examples were given. It was found that the natural frequencies and the corresponding mode shapes of the transverse vibration for roller chain coupled with lumped mass change significantly when the variations of above parameters are considered. With the movement of the chain strand, the natural frequencies present a fluctuating phenomenon, which is different from the uniform chain. The higher the order of mode is, the greater the fluctuating magnitude and frequency are.

To overcome the difficulty on building manually complex models of chain drives, this work proposed a comprehensive methodology to build multibody models of any general chain drive automatically from a minimal set of data [44]. The proposed procedure also evaluated the initial positions and velocities of all components of the drive that are consistent with the kinematic joints or with the contact pairs used in the model. In this methodology, all links and sprockets are represented by rigid bodies connected to each other either by ideal or by clearance revolute

joints. The clearance revolute joint contact was further extended to handle the contact between the chain rollers and the sprocket teeth exact profiles. A suitable cylindrical continuous contact law was applied to describe the interaction on all contact pairs. One of the complexities of the computational study of roller chain drives was the large number of bodies in the system and the dynamics of the successive engagement and disengagement of the rollers with the sprockets. Each time a roller engages or disengages with a sprocket tooth, the number of rigid bodies in contact changes. The search for the contact pairs was recognized as one of the most time consuming task in contact analysis. This work proposes a procedure to specify the contact pairs and their update during the dynamic analysis optimizing the computational efficiency of the contact search. The methodologies adopted result in a general computer program that is applied and demonstrated in a generic chain drive that can be used in industrial machines, vehicle engines or any other type of mechanical system.

Roller chain drives are recognized to be one of the most effective forms of power transmission in mechanical systems [45]. However the mesh between chain and sprocket is generally not a conjugate action. The noise and vibration in such systems can be a problem in the further development and application of this kind of mechanism. Based on the theory of approximately conjugate meshing, a way of simulating the meshing process of roller chain drive was developed to realize sprocket virtual machining. The principle of sprocket virtual machining and envelope molding is regarding the roller as cutter to machine sprocket rough. The profiles of sprocket teeth are the envelope of cutter when it moves on the rough. Virtual machining and design process of sprocket profile was investigated using secondary developing technology of AutoCAD. The dynamic model of roller chain drive mechanism with new sprocket was built by using multi-body dynamic techniques. The meshing process of roller chain drive can be accurately simulated by this model. Simulation analysis shows that the tension between chain links is decreased and the chain/sprocket meshing impact is reduced by applying new sprocket.

2.3 Summary of Literature Review.

Mathematical Models	Study of Polygonal Effect due to change in instanteneous centre during rotation of roller engaged with sprocket [8], [9], [10], [11].
	Mechanics of roller-sprocket impact, various relative impact velocities were derived [8].
	Determined quasi-static chain and sprocket load distributions [16], [17], [18] ,[19].
	Inertia effects on impact forces in chain drives [12], [13].
	An approximate kinematic analysis of the roller chain drive [21].
	Lumped mass dynamic model based on Lagrange's equation to study chain drive vibrations [22], [23].
Physical Models	Fundamental loads on chain drives using an optical strain gage. [6]
	Model of the roller-sprocket contact mechanics that allowed the first determination of actual pressure angles [26], [27].
	Kinetostatic analysis of a roller drive was performed [36].
	Construction and instrumentation of a machine to measure tension and impact forces in roller chain drives [35].
Simulation Models	Computer-aided analysis for the selection of roller chain drives [32].
	Investigation to study the optimization of the chain drive system on sports motorcycles [37].
	A model of a roller-chain drive was developed and applied to the simulation and analysis of roller-chain drives of large marine diesel engines [39].
	The modal characteristics of the transverse vibration of an axially moving roller chain coupled with lumped mass were analyzed [423.
	Simulating the meshing process of roller chain drive [45].

2.4 Gaps in Literature review.

Many mathematical models have been build up which have helped in determining the key values in the design of chain drive. Some of them have been useful in determining the dynamic behaviour of the drive. But still, those models failed to show the continuous behaviour of drive under action. Physical models had their own significance, in these models, practically working machines were made, test-rigs and working models were made which gave us a very good visualization of how did the chain drive actually worked. Test-rigs help in evaluating that the chain-drive meets a desired test value or not. It had become easy so as to find the faulty samples which did not performed to the desired limit. Now the scenario is such that, for a sample to be tested on a test-rig, it has to be manufactured. For companies with mass production, it is very difficult to manufacture new products daily. Even to vary a single dimension of an existing product, they have to change many die-sets, change many manufacturing units with increased cost and lead time. And many a times it happens that the new product manufactured is such that the existing testing rig may not be suitable to test the new product and requires change in machine and/or method.

With the help of simulation software's, now-a-days it has become easier to solve this multiple 'what-if' scenario much easily and effectively with the help of Finite Element Analysis. From the detailed literature survey it has been observed that very less number of works has been reported on FEM analysis of drive chains. FEM modelling of drive chain needs a special attention since the behaviour of chain elements during static testing (like tensile testing of few link elements) and dynamic testing (which needs simulation of full chain with actual running condition assembled with the sprockets) for testing of fatigue life and endurance limit. Thus a lot of scope is observed and the real need is felt for the development of FE model for drive chain elements that can simulate and replace the long mechanical testing like tensile, endurance and fatigue testing especially during the new product development.

2.5 Problem Formulation

Observing the gaps in literature, development of a complete model for FE analysis of the drive chain is attempted to develop. The model is first planned to develop for a transient structural analysis for tensile testing. Using the results of the tensile test, models for endurance test and fatigue test of roller chains is planned to develop. The results of these models are validated with the results of standard one as the practical use. The same has been collected from a leading drive chain manufacturing company in North India. Different types of contacts are also tested after studying all the types of contacts and effect of changes in boundary condition, parametric models has been made for the different type of tests and validated. Using these parametric models, effect of dimensional changes meant for chain weight reduction has been tested not sacrificing the strength and performance to a great extent.

Chapter 3 METHODOLOGY

In this chapter the methodology followed to build model for tensile test, fatigue test and endurance test has been discussed. The procedure followed to build the CAD models, boundary conditions applied to different tests, material data used and the mode of contact in between the mating parts has been discussed. Before starting the different tests, some pilot test had been done in order to properly understand the different types of contacts and their effect on the test, also seamed bush and seamless bush were compared.

3.1 Basic Steps followed in present simulation study.

3.1.1 CAD Model Generation

Pro-Engineer and ANSYS were used to create modeling and simulation. Part Modeling shows how to draft a 2D conceptual layout, create precise geometry using basic geometric entities, and dimension and constrain geometry. It also shows how to build a 3D parametric part from a 2D sketch by combining basic and advanced features, such as extrusions, sweeps, cuts, holes, slots, and rounds.

Model for tensile test was easy to be created and is shown in Figure 3.2 and moreover, a parametric model could be easily developed which rejected the need of external data files. However the model for endurance and fatigue testing is a complex model, had a lot of geometrical operations and needs special care. The developed model is shown in Figure 3.1.

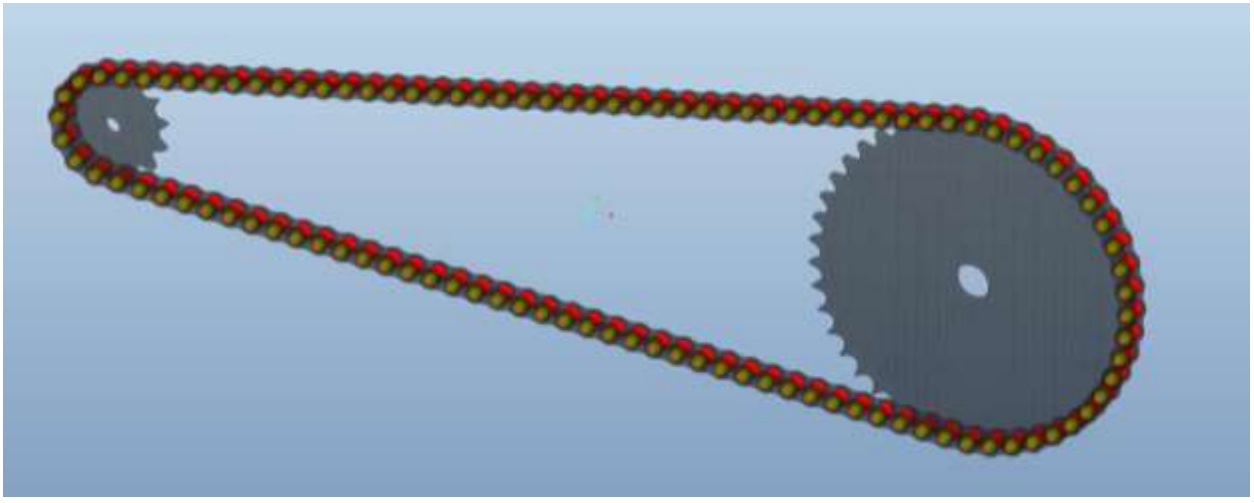

Figure 3.1: Assembly created for Endurance and Fatigue study.

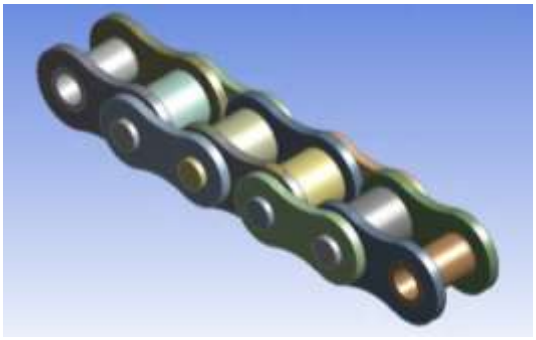

Figure 3.2: Assembly created for Tensile Study.

In the given dimensions, interference was observed at many points which was removed for ease of analysis (shown in Figure 3.3 and Figure 3.4).

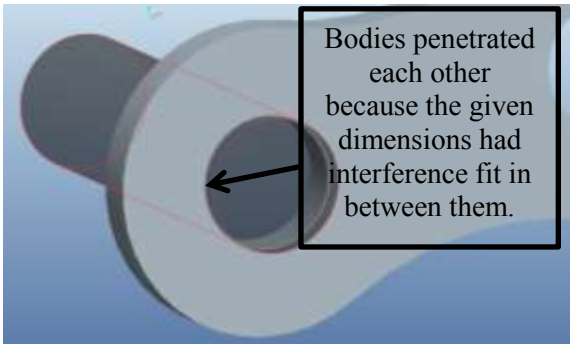

Figure 3.3: Body Interference.

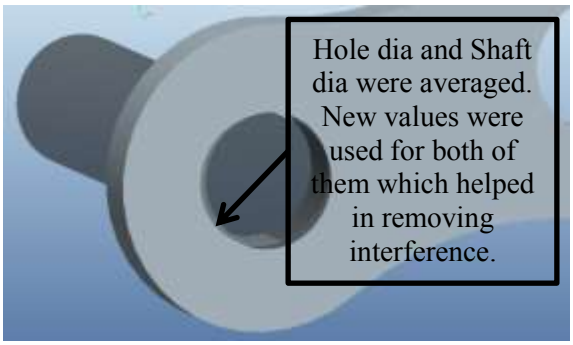

Figure 3.4: Average Hole Dimensions to Remove Interference.

After creating the parts, assembly was created and the necessary types of contacts were defined as shown in Figure 3.5.

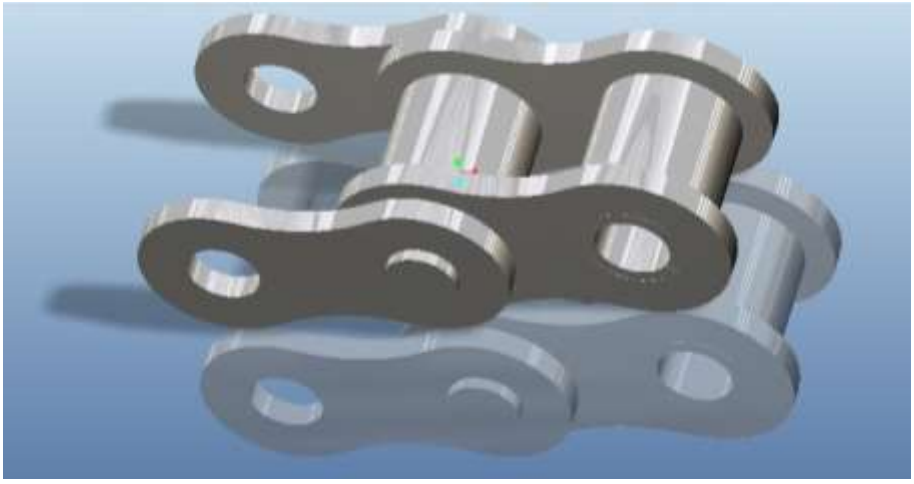

Figure 3.5: Assembly Visualization (1 link).

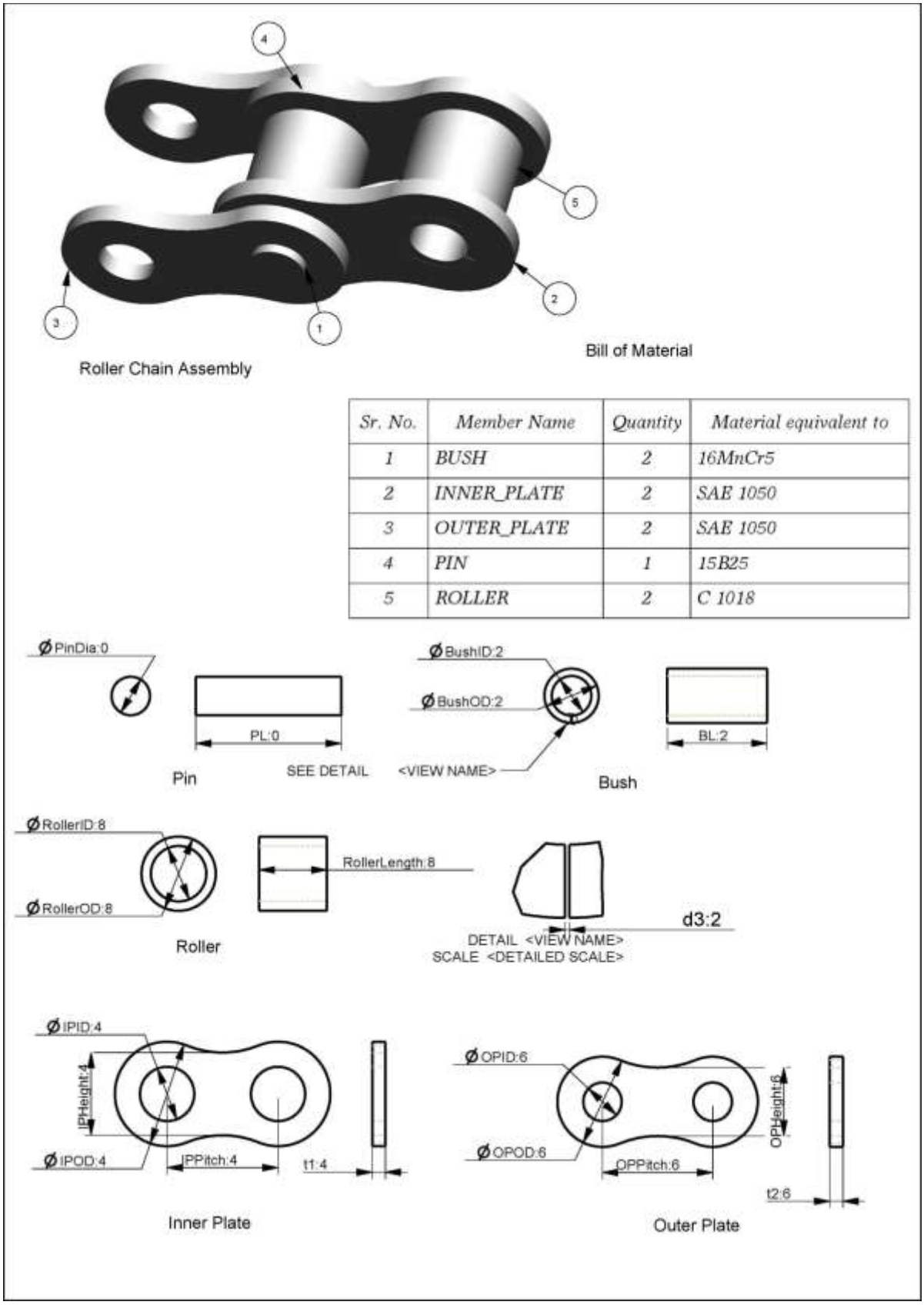

Sr. No.	Member Name	Quantity	Material equivalent to
1	BUSH	2	16MnCr5
2	INNER_PLATE	2	SAE 1050
3	OUTER_PLATE	2	SAE 1050
4	PIN	1	15B25
5	ROLLER	2	C 1018

Figure 3.6: Geometric details of all chain elements.

3.1.2 Editing the Geometry for applying boundary conditions

The geometry file modified so that required contact regions can to be created. Trim the faces so as to make a face which is of our interest (as shown in Figure 3.8).

Problems with current Geometry:-

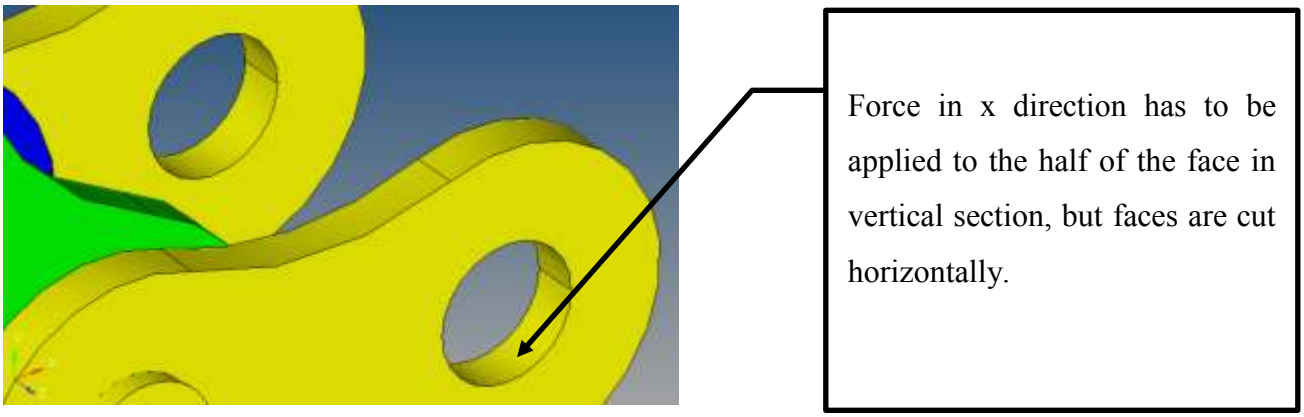

Figure 3.7: Assembly imported for analysis purpose.

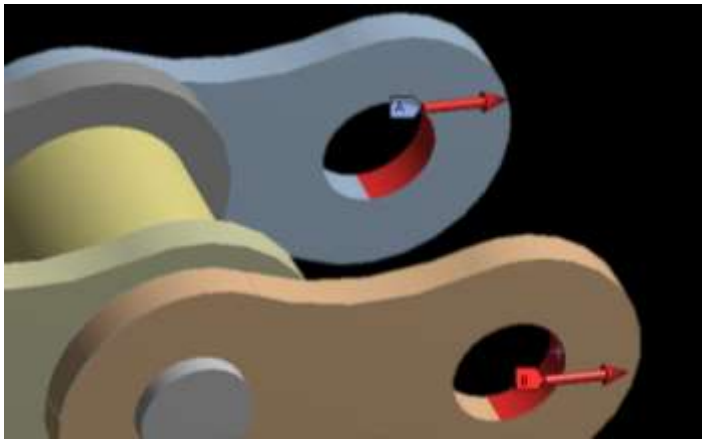

Figure 3.8: Assembly after cutting faces and applying forces.

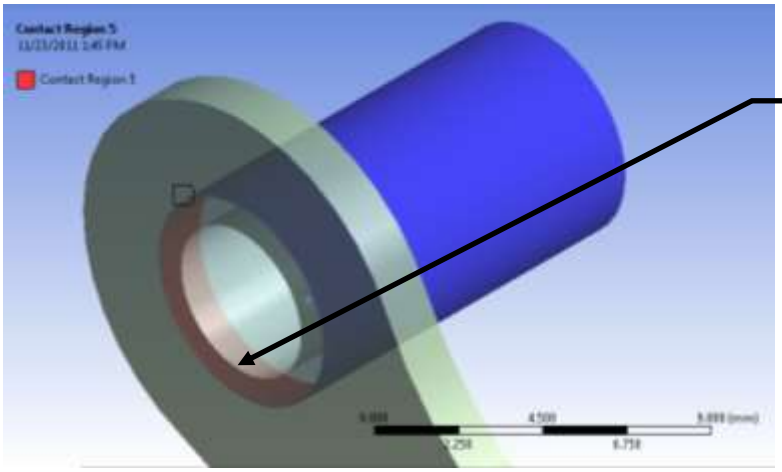

Contact occurs in between the common volume of both the interacting volumes. So the faces were trimmed to create a common face.

Figure 3.9: Default Contact Region.

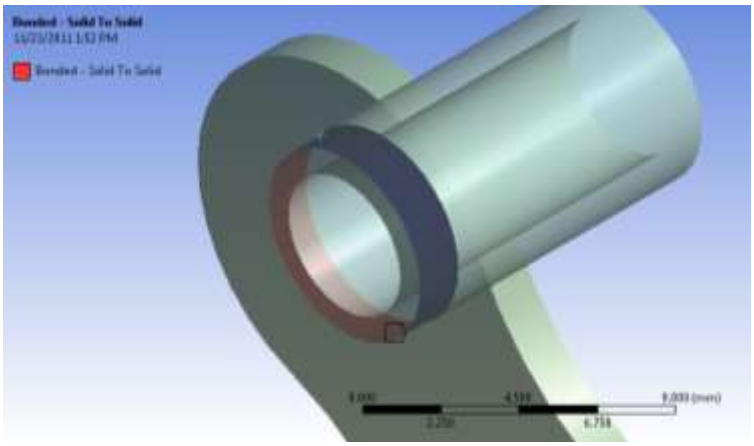

Figure 3.10: Contact Region after Trimming Faces.

Many such contact faces were trimmed as shown in Figure 3.9 and Figure 3.10 and the final model is shown Figure 3.11.

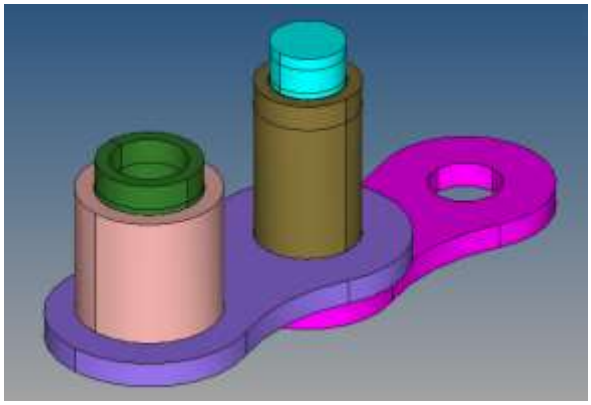

Figure 3.11: Final Model of Assembly showing Faces Cut.

3.1.3 Post-Processing

Standard FEM packages has the capabilities to solve problems in the field of :

- Structural
  - Linear
  - Nonlinear
    – Material, Geometric, Contact
  - Dynamics
    – Modal Harmonic Transient Dynamic Spectrum Random Vibration
    – Modal, Harmonic, Dynamic, Spectrum, – Explicit Dynamics.
- Thermal
  - Steady Transient
- Fluid (CFD, Acoustics, and other fluid analyses)
- Low- and High-Frequency Electromagnetics
- Coupled Field.

3.2 Material Data

The components used for chain were being made of different materials, the component name and their corresponding material is already given in Figure 3.6: Geometric details of all chain elements. Different heat treatment processes are applied on the components so as to enhance its different properties. Each component goes through three stages i.e. acquiring raw material, hardening it till the desired level and then tempering to get the final desired level of strength (shown in Figure 3.12).

Figure 3.12: Stages occurred in component preparation.

Components from each stage were acquired from a company in North India manufacturing chains. The tensile test for determining the Tensile Strength, Young's Modulus and the Stress v/s Strain cure was performed for each stage and the results were evaluated. The components from the first stage i.e. the raw material were easily tested on the Ultimate Testing Machine in the university.

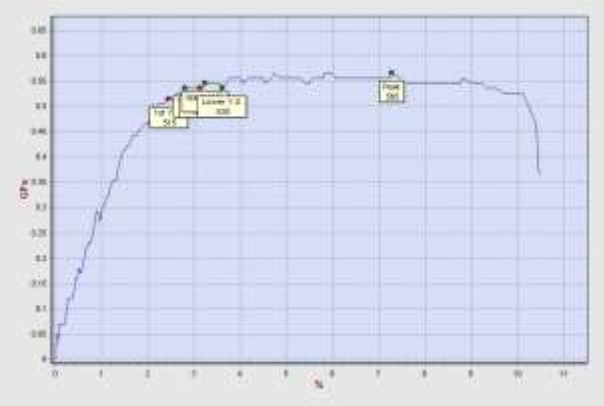

Figure 3.13: Stress v/s Strain Graph for Bush.

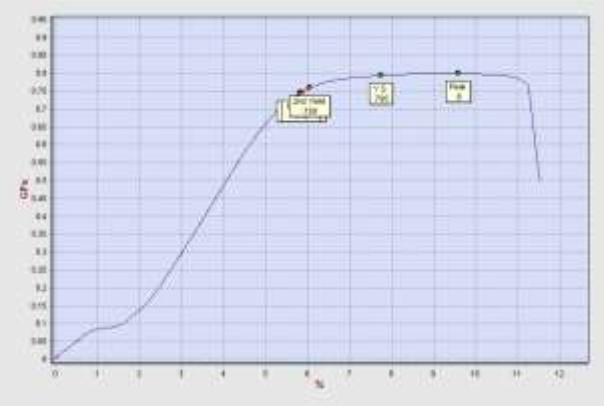

Figure 3.14: Stress v/s Strain Graph for Outer Plate.

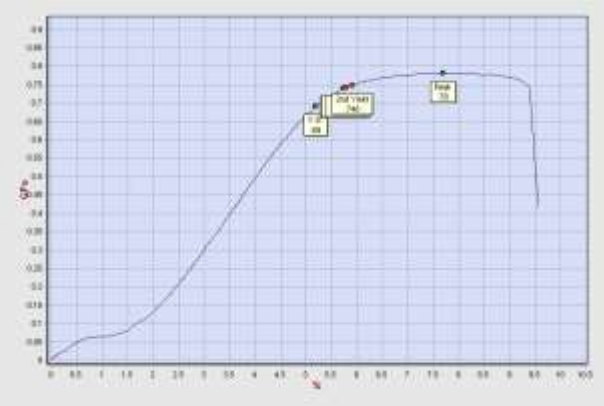

Figure 3.15: Stress v/s Strain Graph for Inner Plate.

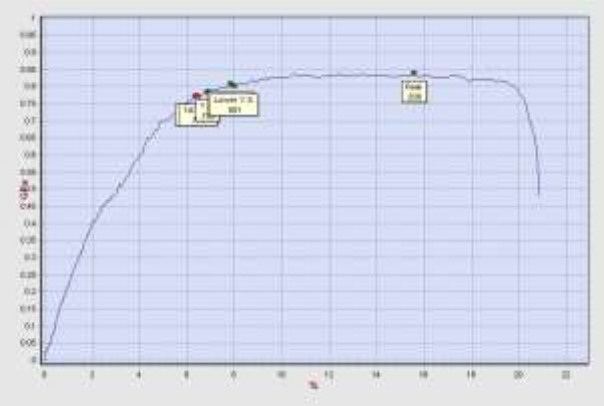

Figure 3.16: Stress v/s Strain Graph for Pin.

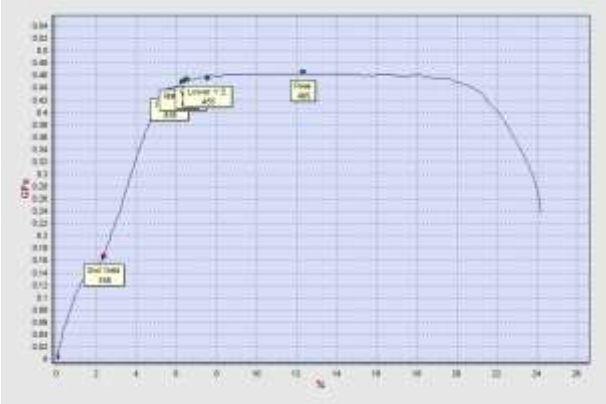

Figure 3.17: Stress v/s Strain Graph for Roller.

Components from the raw stage could be easily tested on the machine. But for hardened stage, it was difficult to test them as they began to slip from the jaw of machine. Hydraulic clamping along with different sets of grippers was used, but as the surface became hardened, it continued to slip. Components from the final stage were given to a laboratory in Ludhiana. Three out of five components (Outer Plate, Inner Plate and Roller) could be successfully tested and the testing results are shown in Table 3.1.

Table 3.1: Tensile Strength of different Components.

Component Name	**Outer Plate**	**Inner Plate**	**Roller**
Tensile Strength (MPa)	1339.04	1385	631.02

For the other components (Pin and Bush) ASTM standard A370-11a was used. The manufacturer had provided us with surface hardness and core hardness. Hardness was converted into its corresponding tensile strength from Table 2. The Poisson's ratio and Young's modulus for the material remains same irrespective of the heat treatment, hence their values were taken from material samples as available in matweb and the values are displayed in Table 3.2 [46].

Table 3.2: Material Properties.

Component	**Hardness**	**Tensile Strength (MPa)**	**Poisson's Ratio** [46]	**Young's Modulus (MPa)** [46]
Inner Plate	43 (HRc)	1337	0.29	2.00E+05
Outer Plate	43 (HRc)	1337	0.29	2.00E+05
Bush	430 (Hv)	1366	0.29	2.05E+05
Roller	410 (Hv)	1303	0.29	2.00E+05
Pin	455 (Hv)	1444	0.29	2.05E+05

Class of Material	Material Effects
Metals	Elasticity Plasticity Isotropic Strain Hardening Kinematic Strain Hardening Isotropic Strain Rate Hardening Isotropic Thermal Softening Ductile Fracture Brittle Fracture (Fracture Energy based) Dynamic Failure (Spall)
Concrete / Rock	Elasticity Porous Compaction Plasticity Strain Hardening Strain Rate Hardening in Compression Strain Rate Hardening in Tension Pressure Dependent Plasticity Lode Angle Dependent Plasticity Shear Damage / Fracture Tensile Damage / Fracture
Soil / Sand	Elasticity Porous Compaction Plasticity Pressure Dependent Plasticity Shear Damage / Fracture Tensile Damage / Fracture
Rubbers / Polymers	Elasticity Viscoelasticity Hyperelasticity
Orthotropic	Orthotropic Elasticity

Figure 3.18: Different material models available for simulation purpose.

3.3 Various Models to Simulate Depending upon type of Test.

Depending upon the type of test performed on the Chain, various models have been made and the model whose output is close to the required values is selected. Modeling and Simulation has to be done for the following tests:-

1. Tensile Test
2. Endurance Test.
3. Fatigue Test.

In this chapter, each type of test, its modeling and its simulation results have been studied. While simulating the models, there were a number of options which had to be checked as to which option would result into correct output. Hence some Pilot Tests have been performed.

3.4 Pilot Tests

To determine contact in between two bodies, there are a number of contact types that may be defined for a practical case like: frictional, bonded, frictionless, rough etc. Each type of contact pair results into different output and hence has to be wisely used. At some places choosing a contact which can reduce the computing time and give an approximate result is good, but at some places exact contact has to be selected so as to have an exact result. The only place where the question of selecting proper contact was in between Pin and Bush, Bush and Roller. So bonded contact and frictional contact were checked as to which would give proper result and did the result really changed if these two contacts were swapped.

3.4.1 Bonded contact v/s Frictional contact.

Bonded is the default configuration and applies to all contact regions (surfaces, solids, lines, faces, edges). If contact regions are bonded, then no sliding or separation between faces or edges is allowed. Think of the region as glued. This type of contact allows for a linear solution since the contact length/area will not change during the application of the load. If contact is determined on the mathematical model, any gaps will be closed and any initial penetration will be ignored.

In frictional contact, the two contacting geometries can carry shear stresses up to a certain magnitude across their interface before they start sliding relative to each other. This state is known as "sticking." The model defines an equivalent shear stress at which sliding on the geometry begins as a fraction of the contact pressure. Once the shear stress is exceeded, the two geometries will slide relative to each other. The coefficient of friction can be any nonnegative value.

Initially a model with one pair of pin and bush was considered as this could be simulated easily and in less time. Roller was ignored. Figure 3.19shows the model used to do the simulation and Figure 3.20 shows the contact region in study.

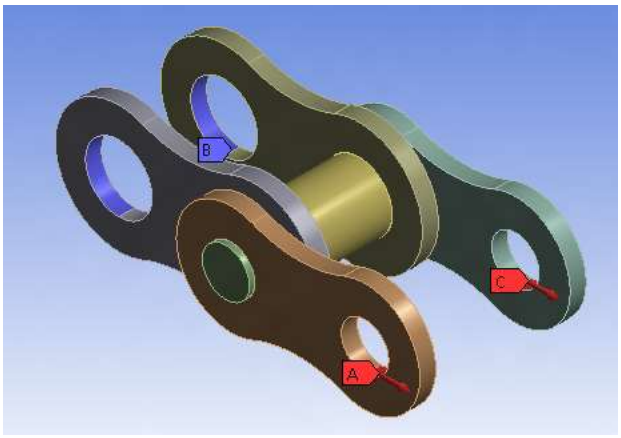

Figure 3.19: Model used to study contacts.

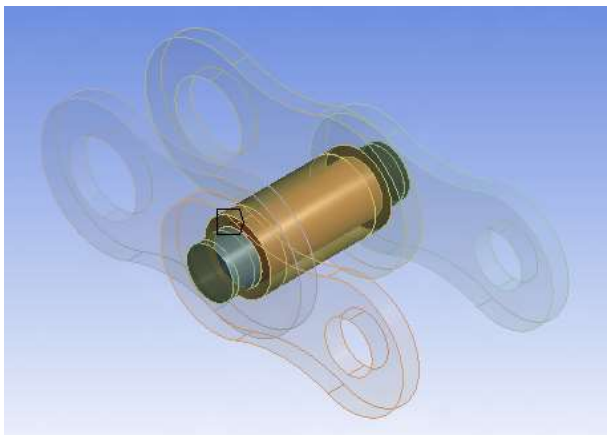

Figure 3.20: Contact region.

Above model was simulated with bonded contact and frictional contact. When bonded contact was used, the model was solved in one iteration. But for frictional contact, as the connection became non-linear because of gap in between them, the model had to be changed from static to transient and then solve it. Few of the output results are compared in the Table 3.3.

Table 3.3: Comparison of Bonded and Frictional Contact.

	Bonded	**Frictional**
Maximum Stress (MPa)	131.12	131.13
Maximum Displacement (mm)	0.00607	0.0668
Number of iterations	01	65

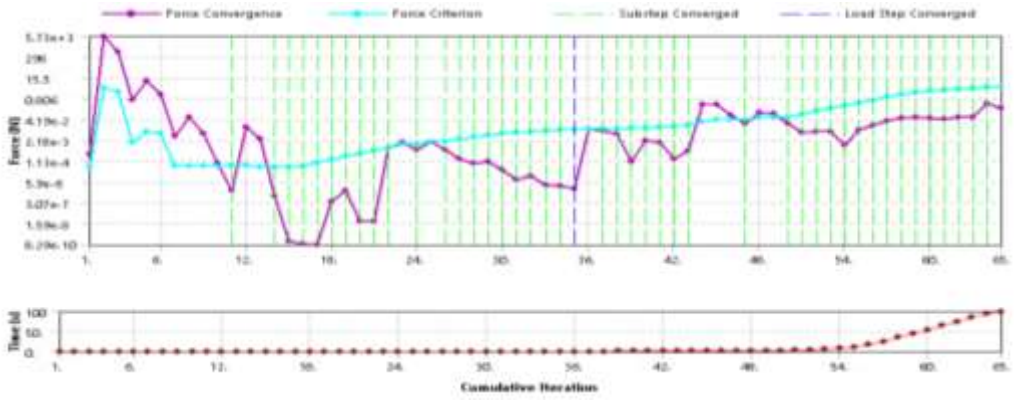

Figure 3.21: Number of iterations required to solve the model using Frictional Contact.

At the first glance, it could be easily commented that the bonded contact gave quicker and nearly same results. Value of equivalent von-Mises stress is same in both the cases. The deformation value is greater in frictional contact, it is due to the gap in between the bodies. If the gap is subtracted from the total deformation, the value becomes same as that of bonded contact.

Even though the computing time is more and the number of iterations required is huge for frictional contact as compared to bonded contact (shown in Figure 3.21), but still frictional contact has capability of giving precise results. Using the contact tool, again both of the contacts are compared. Contact tool can be used to evaluate Status, Frictional Stress, Pressure and Sliding Distance between any contacting bodies. Pressure and Stress results based on this contact tool have been compared again.

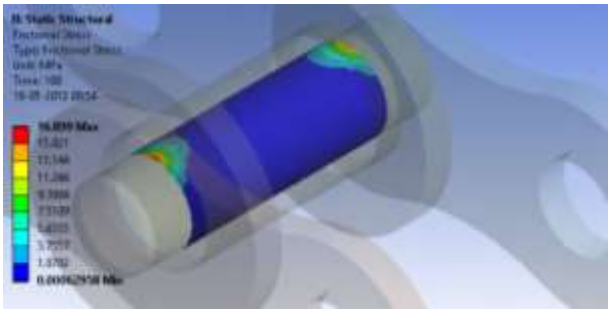

Figure 3.22: Frictional stress with bonded contact in use.

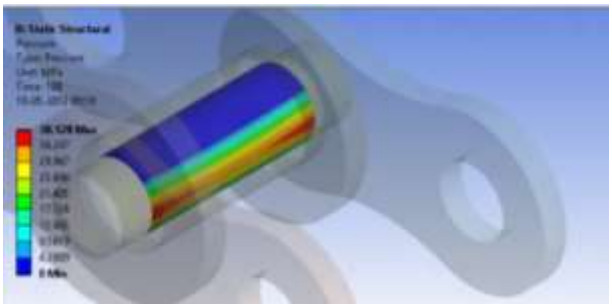

Figure 3.23: Frictional stress with frictional contact in use.

As it can be clearly seen in the Figure 3.22 and Figure 3.23, frictional contact gave the exact areas where maximum stress is developed according to the loading condition. In bonded contact, maximum stressed area is not along the line of contact, it is because both the areas are bonded together. Also frictional contact helped in easily visualizing the exact way the contact happened. Even though the analysis took 65 iterations, the different values which could be extracted from frictional contact made its use worth where exact contacting details were required. Equivalent body stresses are same in both the cases, but the frictional stresses differ a lot in each case. Hence frictional contact is more superior to bonded contact. For an initial stress value, bonded joint can be used, but for exact and more accurate results, it is preferred to use frictional contact.

3.4.2 Seamed bush v/s seamless bush.

Currently the bush used in current chain drive is manufactured by rolling a flat strip, hence it had a seam in between as shown in Figure 3.24. The place as where did seam got fitted in the assembly was studied by changing the angle. Finally comparison was made in between the seamed bush and seamless bush.

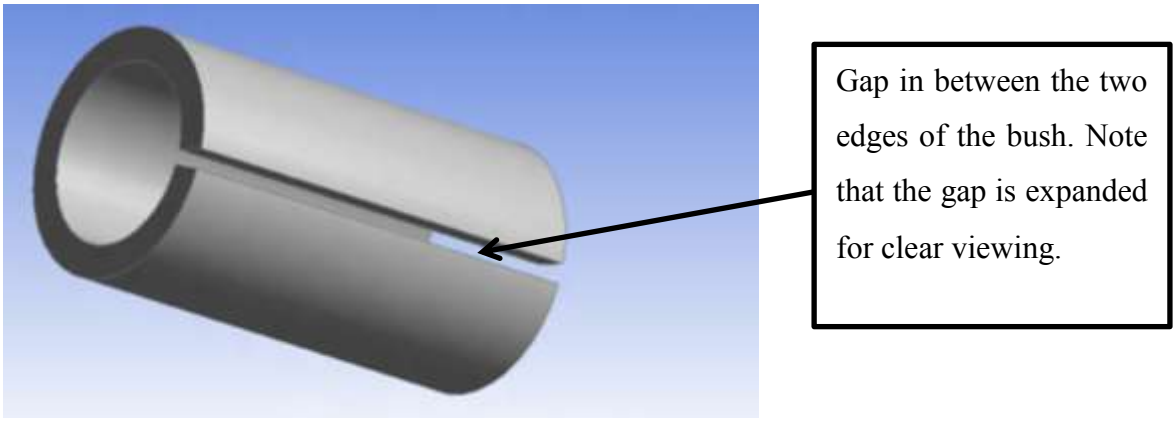

Figure 3.24: Seamed bush used in current drive chain.

While assembling the chain, there is no particular orientation of the bush. The seam in the bush gets fitted at any angle. An attempt to simulate the different orientation of the seam and the corresponding stresses was made. Seamless bush gave the minimum contact stresses and is hence preferred.

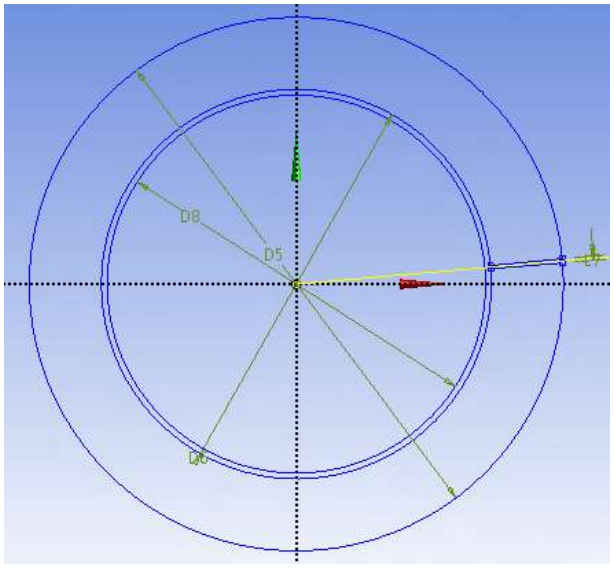

Figure 3.25: Cross Section of Pin and Bush.

The line shown in yellow colour in the Figure 3.25 is the line with which the seam angle is measured. The degree at which this line is inclines was varied and corresponding contact stresses were calculated. In table 3.4, the values in degree are measured from the x axis (shown in red colour in Figure 3.25).

Table 3.4: Variation of seam and corresponding Contact Stresses.

Degree of Inclination.	Equivalent Stress (MPa)	Contact Frictional Stress (MPa)	Contact Pressure (MPa)
0°	1484.8	175.89	1023
1°	1485.2	181.61	1043.8
2°	1488.4	191.69	1068.9
180°	1486.7	163.43	842.16

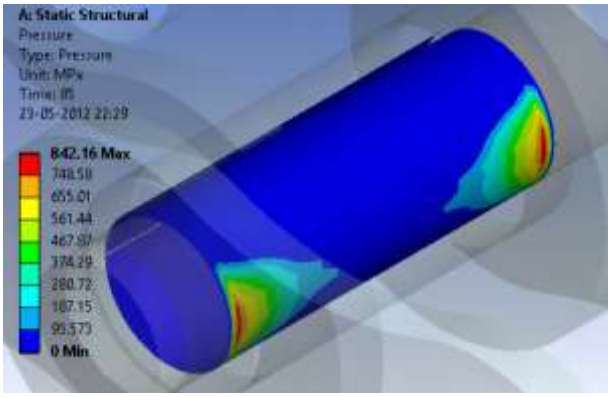

Figure 3.26: Contact Pressure variation when seam is at 180°.

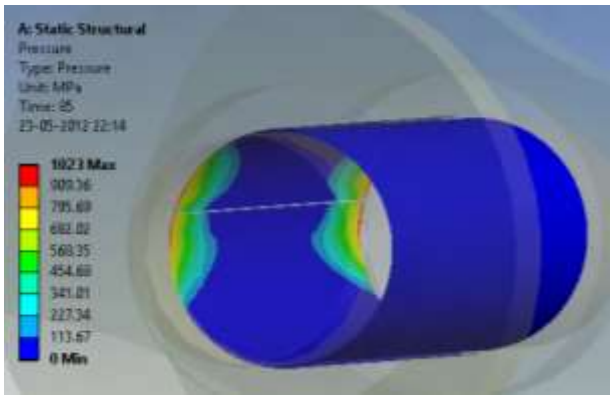

Figure 3.27: Contact Pressure variation when seam is at 0°.

3.5 Tensile Test

Tensile testing of roller chains is already discussed in section 1.7.1. Two cases occur depending upon which face to be kept as fixed or apply force.

Back face shown as region 1 can be fixed and force in positive x axis (as in the co-ordinate system in the Figure 3.28) can be applied to region 2. And second model can be generated by applying force on region 1 in negative x-axis and fixing the region 2.

Figure 3.28: Different Regions Based on Boundary Condition.

Both the types of configurations are shown in Figure 3.29and Figure 3.30 respectively and their names are also mentioned.

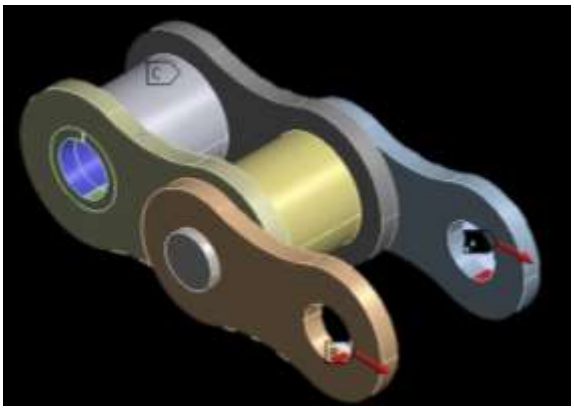

Figure 3.29: Configuration considered as 'Case 1'.

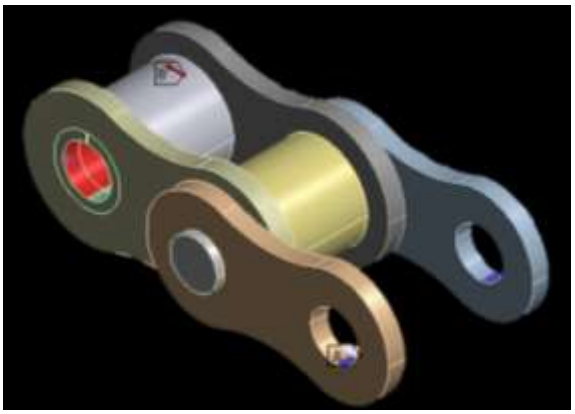

Figure 3.30: Configuration considered as 'Case 2'.

3.5.1 Various Models to Simulate Depending upon type of Connections

Contact between two objects is one of the most frequently encountered phenomena in engineering analysis. For a complete chain assembly, many types of joints and contacts are developed after the elements are assembled. This entirely depends on the fact that how these elements are joined with each other, like: with clearance gap, with press fitting etc. To incorporate these issues in modelling, different types of connections are discussed in terms of contact region and joints.

A. Contact Region

The faces of contacting bodies were picked individually and specify them as contact face or target face. A set of contact face and target face make a contact pair. Different types of contacts are explained below:

a. **Bonded:** This is the default configuration and applies to all contact regions (surfaces, solids, lines, faces, edges). If contact regions are bonded, then no sliding or separation between faces or edges is allowed. Think of the region as glued. This type of contact allows for a linear solution since the contact length/area will not change during the application of the load. If contact is determined on the mathematical model, any gaps will be closed and any initial penetration will be ignored.

b. **No Separation:** This contact setting is similar to the bonded case. It only applies to regions of faces (for 3-D solids) or edges (for 2-D plates). Separation of faces in contact is not allowed, but small amounts of frictionless sliding can occur along contact faces.

c. **Frictionless:** This setting models standard unilateral contact; that is, normal pressure equals zero if separation occurs. It only applies to regions of faces (for 3-D solids) or edges (for 2-D plates). Thus gaps can form in the model between bodies depending on the loading. This solution is nonlinear because the area of contact may change as the load is applied. A zero coefficient of friction is assumed, thus allowing free sliding. The model should be well constrained when using this contact setting. Weak springs are added to the assembly to help stabilize the model in order to achieve a reasonable solution.

d. **Rough:** Similar to the frictionless setting, this setting models perfectly rough frictional contact where there is no sliding. It only applies to regions of faces (for 3-D solids) or edges (for 2-D plates). By default, no automatic closing of gaps is performed. This case corresponds to an infinite friction coefficient between the contacting bodies.

e. **Frictional:** In this setting, two contacting faces can carry shear stresses up to a certain magnitude across their interface before they start sliding relative to each other. It only applies to regions of faces. This state is known as "sticking." The model defines an equivalent shear stress at which sliding on the face begins as a fraction of the contact pressure. Once the shear stress is exceeded, the two faces will slide relative to each other. The coefficient of friction can be any non-negative value.

Advantages of bonded contact:

- Faster solutions since there are no contact convergence issues. Convenient for a quick analysis of assemblies.
- Small-deflection cases can be run as linear analyses with one substep and one equilibrium iteration.
- Also allows large deflection analyses.

Seven main steps:

a. Create or import the geometry.
b. Mesh all of the contacting bodies. (Required for step 3.)
c. Create the contact pair.
d. Specify the analysis type and solution controls.
e. Apply loads and boundary conditions.
f. Save the database.
g. Solve and review results.

Above steps were followed and contact regions for the chain assembly was created.

B. Joints

A joint is used to define conditions for reference and mobile pairs that make up a joint. Two types of joint configuration are available, Body-Ground and Body-Body. Body to Body Joints were used to define the assembly. Types of joints available are entailed in Table 3.5.

Table 3.5: Types of Joints.

Sr. No.	Type of Joint	Constrained degrees of freedom
1	Fixed Joint	ALL
2	Revolute Joint	UX, UY, UZ, ROTX, ROTY
3	Cylindrical Joint	UX, UY, ROTX, ROTY
4	Translational Joint	UY, UZ, ROTX, ROTY, ROTZ
5	Slot Joint	UY, UZ
6	Universal Joint	UX, UY, UZ, ROTY
7	Spherical Joint	UX, UY, UZ
8	Planar Joint	UZ, ROTX, ROTY
9	Bushing Joint	None
10	General Joint	Fix All, Free X, Free Y, Free Z, and Free All

3.5.2 Models based on Connection Types and Model Configuration

Each type of connection i.e. contact region and joints were applied to the assembly. Still the two sub-cases on each type of connection based on the direction of force applied were simulated and the respective results were evaluated (Table 3.6).

Table 3.6: Results of each type of Case.

Sr. No.	Type of Connection	Model Configuration	Maximum Stress (MPa)	Maximum Deformation (mm)	Weakest Member
1	Contact – Bonded	Case 1	225.87	0.01886	Inner Plate
2	Contact – Bonded	Case 2	310.23	0.01068	Inner Plate
3	Joints	Case 1	213.85	0.008914	Outer Plate
4	Joints	Case 2	169.52	0.005046	Outer Plate

Maximum stress can be seen in the model no 2. Hence, an assembly with Contact type of connection and Bonded Contact Region is selected.

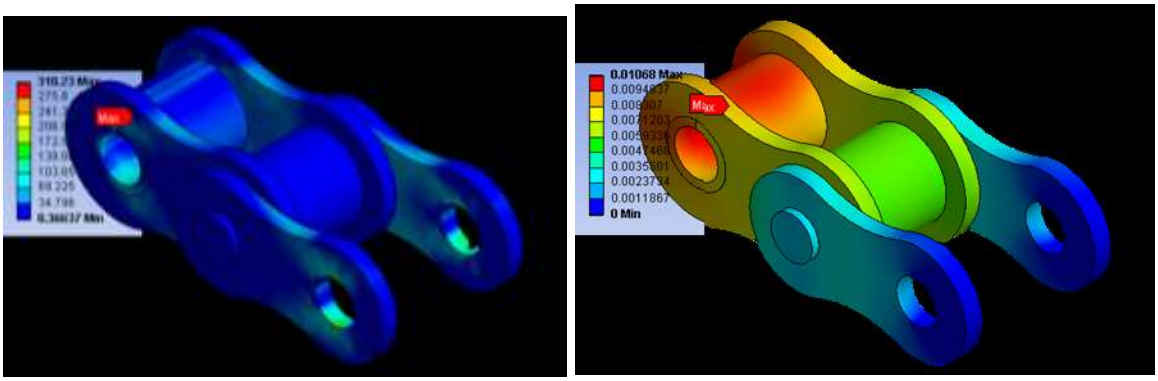

Figure 3.31: Stress Distribution (Left) and Deformation (Right) using Coarse Mesh.

3.5.3 Changing Mesh Type for Precise Results.

A various type of Mesh levels are available. Initially, a model with coarse mesh is modeled and basic results are calculated. Once the model is finalized, higher amount of discretization can be done and more accurate result can be obtained. Use of Proximity and Curvature (P&C) enables a higher amount of discretization as and where required based on the geometric variations. The effect of change of mesh type is studied from Figure 3.32 to Figure 3.37 and the results are shown in Table 3.7.

Table 3.7: Results based on Mesh Type.

Sr. No.	Mesh Type	Maximum Stress (MPa)	Maximum Deformation (mm)	Weakest Member
1	Coarse	310.23	0.01068	Inner Plate
2	Medium	325.49	0.010875	Outer Plate
3	Fine	477.34	0.0108	Inner Plate
4	P&C, Coarse	454.06	0.010941	Outer Plate
5	P&C, Medium	415.08	0.010893	Outer Plate
6	P&C, Fine	453.04	0.010928	Outer Plate

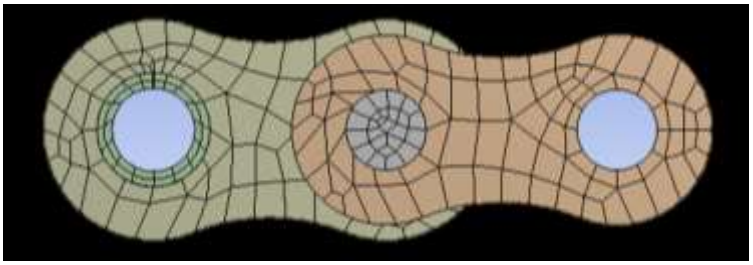

Figure 3.32: Coarse Mesh..

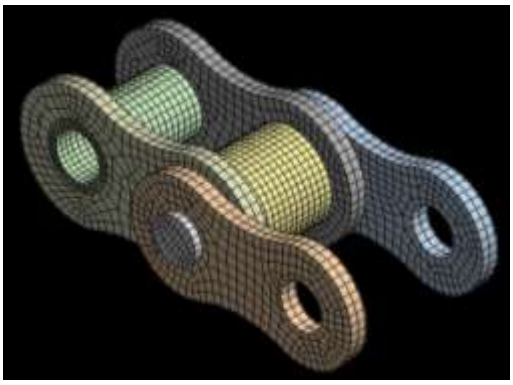

Figure 3.33: Medium Mesh.

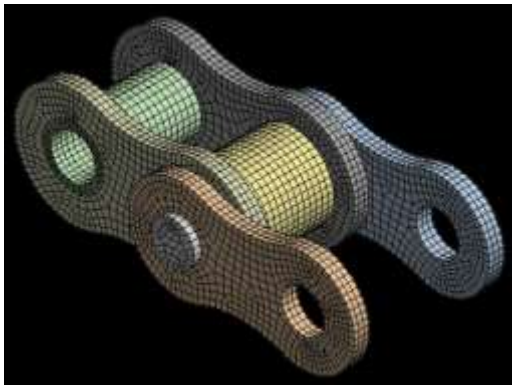

Figure 3.34: Fine Mesh.

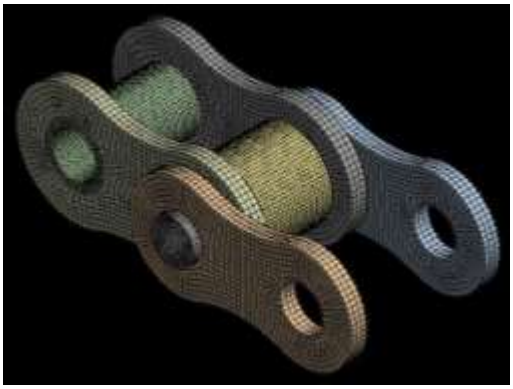

Figure 3.35: Coarse Mesh with P&C.

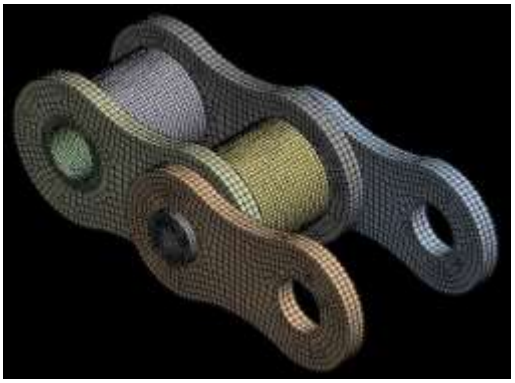

Figure 3.36: Medium Mesh with P&C.

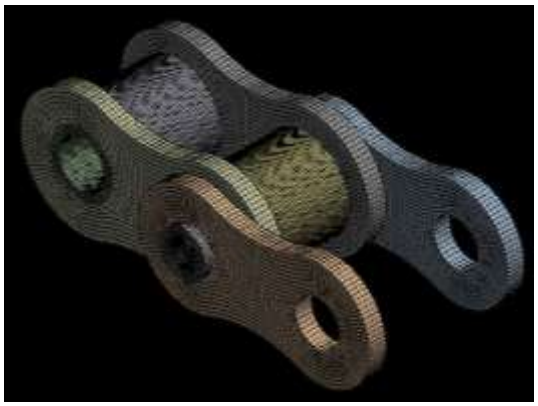

Figure 3.37: Fine Mesh with Proximity and Curvature.

3.5.4 Generating an Optimum Model.

After checking a particular model for its boundary conditions, connections and mesh type, the results of the model were checked by the data as available from the practical tests in the company. Now since the boundary condition and connection types are set. The only variable remains, the number of links. Also in section 1.7.1, the number of links for a practical tensile test was from 3 to 15. Now the final model will be selected by checking the stress and fracture point from the practical data.

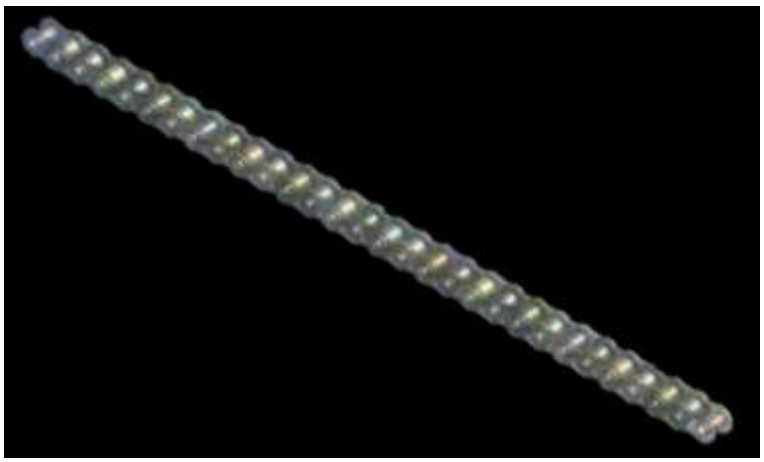

Figure 3.38: 15 Links chain used for Tensile Testing.

A standard 15 links chain used for tensile testing on the Ultimate Testing Machine is shown in Figure 3.40. If the same model was to be built and analysed, it would result in analysing a model made up of 148 bodies. An initial model made consisting 1 link was analysed and checked. The numbers of links were increased if the results did not match. While mounting the chain on the test machine, it could be seen that the inner plates got gripped on the grippers because of greater height, hence the new model was made with start and end plates as the inner plates. Also the inner plates were cut on the four corners where the grippers gripped it.

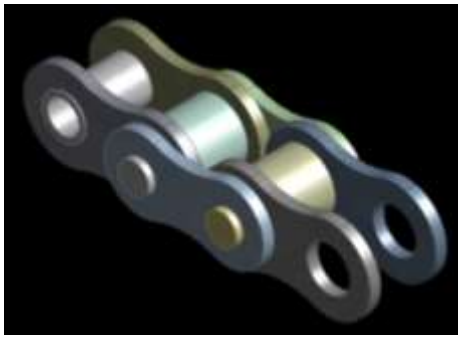

Figure 3.39: Basic model with least number of bodies.

Starting with one link (shown in Figure 3.39), the process of selecting the model begins. Each time the output result of the model disagrees, a new link is added to the assembly and then again the output results are check. Once a model with best output is selected, the different parameters can be changed to study the optimization process. All the required parameters were varied and a best model against the given constraints was selected.

3.6 Fatigue Test

The number of cycles of stress or strain of a specified character that a given specimen sustains before failure of a specified nature occurs is the fatigue life [47]. Fatigue test of chain consists of loading the chain to 38 kgf, then increasing the load to 420 kgf and then repeating the cycle with maximum load as 420 kgf and minimum load of 38 kgf. The no of cycles which the chain can withstand is noted.

For finite element modeling of the above problem, it is needed to first do a structural analysis of the model and then check the fatigue life of the chain. The optimum model created in Tensile Testing was used to do the structural test in which a load of 420 kgf was applied as shown in Figure 3.40.

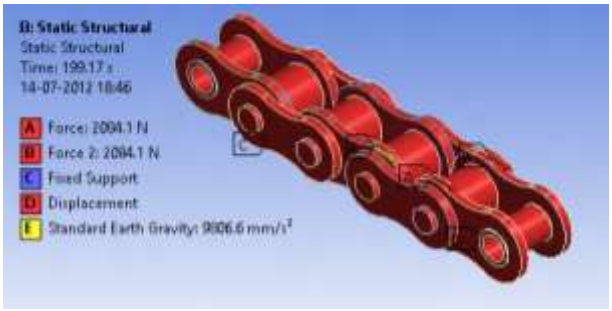

Figure 3.40: Static analysis of Model with load of 420 kgf.

To determine the fatigue life, fatigue properties of the material had to be entered in the Engineering Data. There were three ways to enter the fatigue life.

- Alternating Stress Mean Stress
- Alternating Stress R-Ratio
- Strain-Life Parameters.

- **Alternating Stress**

  The alternating stress, or stress-life (SN), mean curve data can be defined for a mean stress or r-ratio. The Interpolation method (Log-Log, Semi-Log, or Linear) can be defined. The curve data must be defined to be greater than zero.

  - Mean Stress

  Use this definition if experimental SN data was collected at constant mean stress for individual SN curves.

  - R-Ratio

  Use this definition if multiple SN curves were collected at a constant r-ratio. The r-ratio is defined as the ratio of the second loading to the first: r = L2 / L1. Typical experimental r-ratios are -1 (fully reversed), 0 (zero-based), and 0.1 (to ensure that a tensile stress always exists in the part).

  It is possible to define multiple SN curves to account for different mean stress or r-ratio values. The values of mean stress/r-ratio are only important if multiple curves are defined and the SN-Mean Stress Curves correction using experimental data option is chosen in the Fatigue Tool

- **Strain-Life Parameters**

  The following four strain-life parameter properties and the two cyclic stress-strain parameters must have data defined:

  - Strength Coefficient
  - Strength Exponent
  - Ductility Coefficient
  - Ductility Exponent
  - Cyclic Strength Coefficient
  - Cyclic Strain Hardening Exponent

An Alternating Stress Mean Stress model was used to define the fatigue data with two r-ratio values of '-1' and '0'. Log-Log type of interpolation was used to define the data using the values as shown in Table 3.8.

Table 3.8: Alternating Stress Mean Stress Fatigue Data.

r = -1		r = 0	
Cycles	**Alternating Stress (Pa)**	**Cycles**	**Alternating Stress (Pa)**
10000	794808462	10000	677681426.7
14384	770350693.6	14384	656827879.8
20691	748064569.6	20691	637825952.9
29764	727757265.9	29764	620511237.8
42813	709253080.8	42813	604733922.9
61585	692391911.2	61585	590357502.1
88587	677027871.6	88587	577257586.9
127427	663028030.7	127427	565320833.3
183298	650271257.3	183298	554443963.4
263665	638647178.3	263665	544532868
379269	628055220.9	379269	535501794.6
545559	618403739.3	545559	527272605.1
784760	609609228.3	784760	519774099
1128838	601595596.2	1128838	512941396.7
1623777	594293508.1	1623777	506715379.9
2335721	587639782.5	2335721	501042182.8
3359818	581576852.4	3359818	495872717.7
4832930	576052260.1	4832930	491162256.7
6951928	571018204.8	6951928	486870046.1
10000000	566431131.2	10000000	482958947

Once the fatigue data is defined and the model is solved for static structural analysis, fatigue life can be evaluated. Figure 3.41 shows the basic procedure to insert the fatigue tool to calculate the fatigue life of the component.

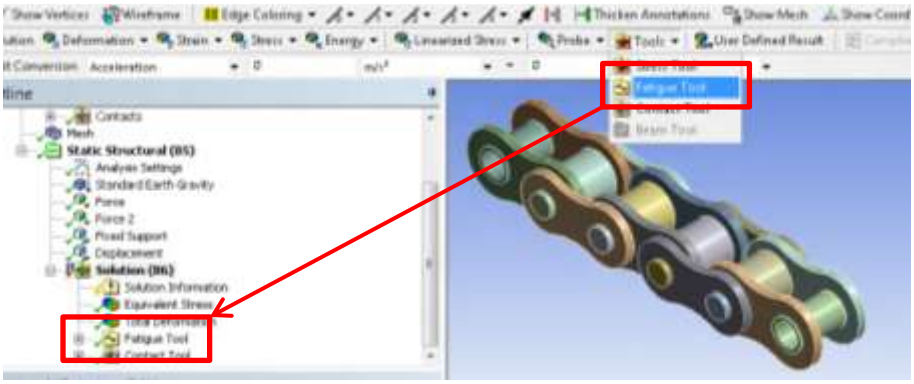

Figure 3.41: Inserting Fatigue Tool.

The fatigue life component of the fatigue tool gives the life of the component analysed.

3.7 Endurance Test

Endurance testing is done to test the chains strength and life when it is being subjected to cyclic loads. The durability and stamina of the chain to resist such uneven loads and perform onto a desired life is being checked. In current test rig the elongation of chain is checked after every 10 hours. Load of 5 KW is applied on the large sprocket so as to simulate the actual loading conditions. Testing continues for 100 hours and elongation of chain is measured.

3.7.1 Connections and Boundary Conditions.

Finite element modeling of a chain having such a huge amount of bodies including contact non-linearities is time consuming as well as a process requiring huge amount of computational resources. While modeling the models for tensile test in Section 3.5 frictional contacts was used so to simulate the actual working of the test. Use of frictional contact gave us the correct result but use more time and computational resources. Simulating a body with 105 links and further each 105 link with both the driven and driver sprocket is really tedious task and requiring gigantic amount of computational resource. Hence bonded connection was used for each links (IP to Bush, OP to Pin) as shown in Figure 3.42. For connection between pin to bush, revolute joint was used (shown in Figure 3.43) which gave the required rotatory degree of freedom between them. Also including revolute joint instead of frictional contact helped in reducing the time and computational resources.

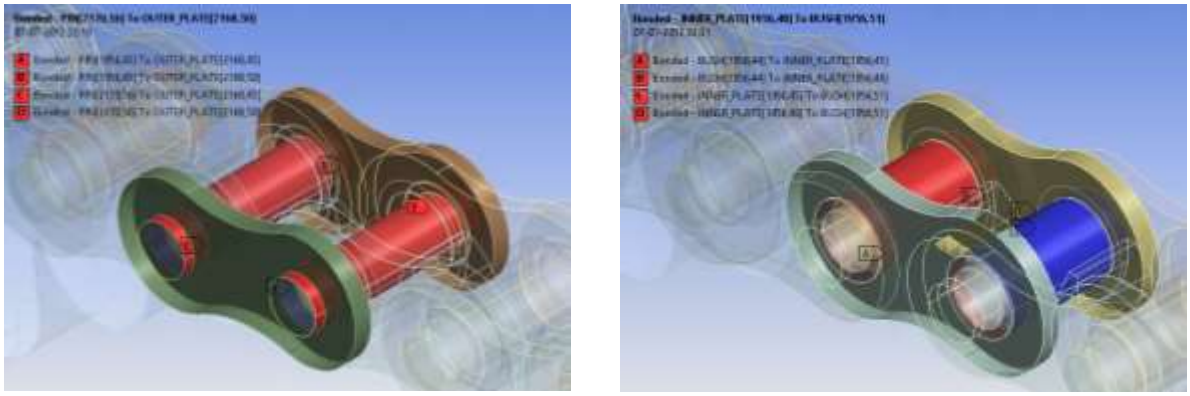

Figure 3.42: Creating sub-assemblies with the help of bonded contact.

Sub-assemblies of pin with outer plate and bush with inner plate were created with bonded connection. In actual fitting also, the pin was press fitted with the outer plate and bush with the inner plate. Giving bonded connection applies a bond between these bodies with which the bodies stick to each other. Only the sticking can be assumed by bonded contact but the initial forces because of press fit were neglected. Now these sub-assemblies were connected to each other with the help of revolute joint. Revolute joint gave only one rotational degree of freedom to the two connecting bodies. Hence the sub-assembly containing pin with outer plate and bush with inner plate were connected to each other. Roller also was given revolute joint with each bush. Revolute joint would be preferred over frictional connection for this particular application as it reduced the degree of freedom automatically and also the computational time and resources.

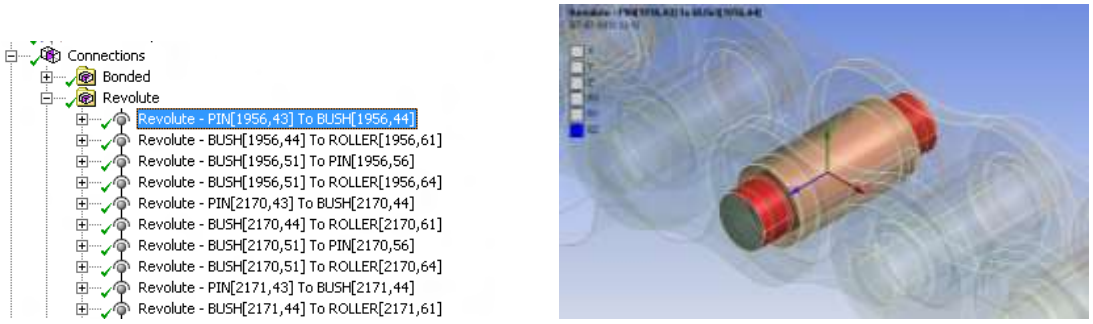

Figure 3.43: Revolute joint between pin and bush.

The only member coming in contact with the sprocket was the roller. As the sprocket rotated, roller came into contact, transmitted the forces to the respective members, and gave the revolute motion and rotational motion to the driven sprocket. Since the contact between the roller and sprocket was present only for a shorter duration of time, frictional contact had to be used at this place because only frictional contact had options in which the contact body keeps on searching

for the target body. All the 105 rollers were given contacts with the driven and driver sprocket. After giving all the necessary connections, a check was made to check if any duplicate contact was present as shown in Figure 3.44.

Figure 3.44: Checking for Duplicate Contacts.

After defining and checking the contacts, rotation to the driver sprocket was given and results were checked.

Based on some initial pilot tests, models had been made which could predict the tensile strength, fatigue life and endurance strength of the chain. All the models made in the previous chapter were analysed here and their results were compared with the actual results. After checking their correctness with the actual value, new models based on dimension change were tested and their tensile strength was evaluated. Fatigue life, damage and safety factor was evaluated successfully. Model for endurance testing was tested. Models based on finite element method were used to depict these test results.

4.1 Tensile Test

4.1.1 Optimum Model Based on Pilot Study.

Model:-

Optimum model (as shown in Figure 4.1) consisted 24 bodies (2 links) having bonded contact in between the inner plate and bush, outer plate and pin; frictional contact in between the pin and bush, bush and roller (as shown in Figure 4.2 with some bodies hidden).

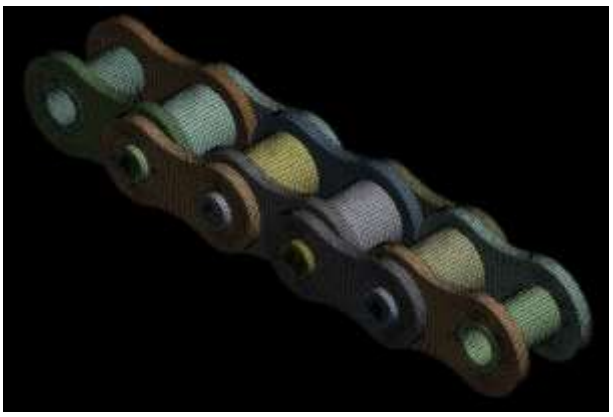

Figure 4.1: Optimum model for Tensile Test.

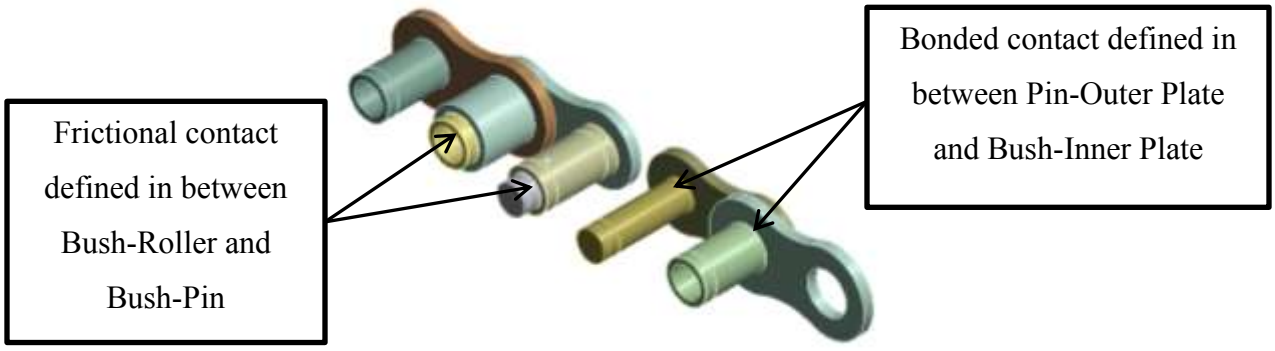

Figure 4.2: Contacts details of the optimal model.

Minimum element size of 0.5 mm was used during the mesh and it was taken into account that there are least 4 elements along the width of each plate. The model generated 449218 nodes and 91242 elements.

Boundary Condition:-

Inner plate being the only body which was being gripped on all the four corners in the gripper, was held fixed on the four corners as shown in Figure 4.3 and a gradually increasing load was applied on the other end of the inner plates as shown in Figure 4.4. Direct load cannot be applied to the model as it had contact non-linearties in it. Hence to fill the initial gap in between the pin and the bush, gravity was applied in the direction of the force so that the bodies can come in contact with each other. After the application of gravity, a load of few Newton's was applied so that the frictional contact would become stiff enough and prevent the penetration of the contacting bodies. The load was then applied with a proper amount and kept gradually increasing till 1900 kgf. Table 4.1 shows the value of load and the time at which the respective step gets complete.

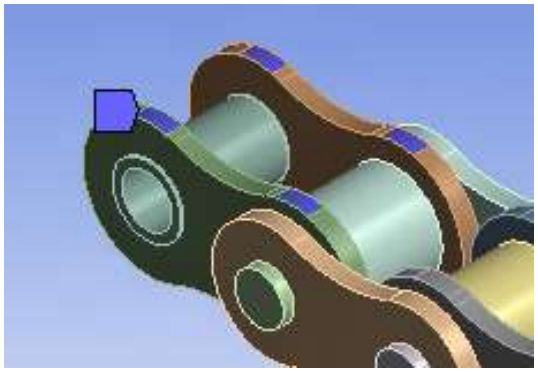

Figure 4.3: Fixed end of the Chain.

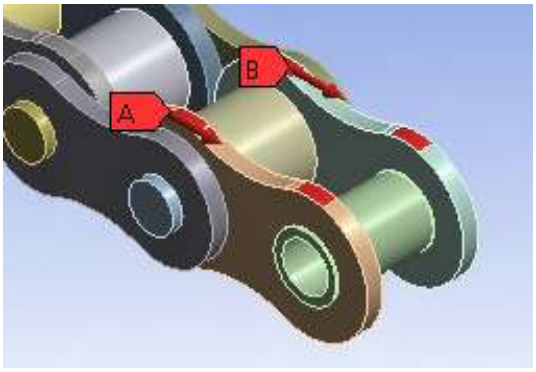

Figure 4.4: Loading end of the Chain.

Table 4.1: Load Step Details (Tensile Test).

Time (s)	Force (N)	Gravity (mm/s^2)
0	0	0
10	0	9806.6
20	4	9806.6
150	2000	9806.6
250	4500	9806.6
350	6000	9806.6
450	8000	9806.6
550	9319.5	9806.6

The force of 9319.5 N was applied on each inner plate which totally made a sum of 18639 N which was applied in two parts namely ‘A’ and ‘B’ as shown in Figure 4.4.

Input Data:-

Material data required for the analysis was given from Table 3.2 which had Young’s modulus, Poisson’s ratio and tensile strength of respective component. To be on a safe side, the maximum stress was not allowed to be greater than 1303 MPa, which is the minimum stress at which a component breaks. Taking the minimum stress at which a component breaks as the maximum allowable stress on the whole chain, the load on the chain was increased and finite element model was checked. To exactly define the elastic and plastic data, the stress v/s strain curve for each component was entered using Multilinear Isotropic Hardening option in the engineering data component.

4.1.2 Results of Optimal Model.

Finite element model showed that the chain would break at a load of 1834 kgf as that actual breakage load of 1850 kgf (Reference from standard manufacturer company).

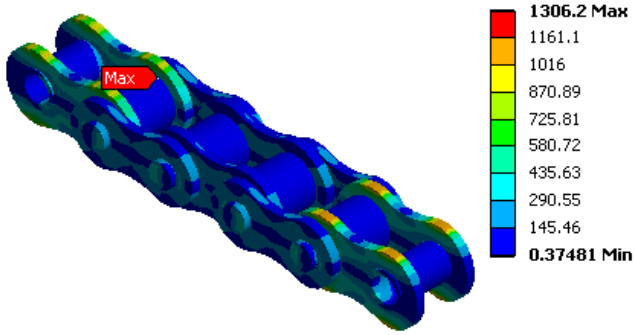

Figure 4.5: Stress variation over the chain (MPa) for the optimal model during tensile test.

Figure 4.5 shows the equivalent von-Mises stress over the entire chain.

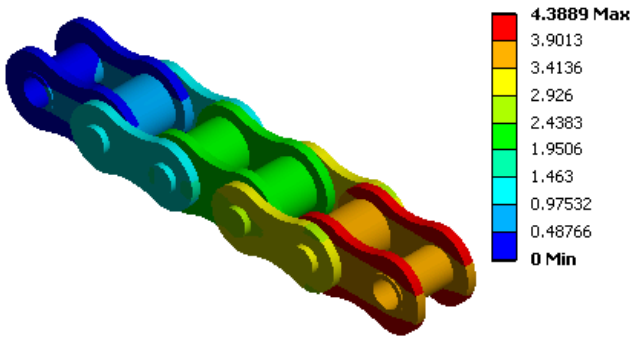

Figure 4.6: Deformation of the chain (mm) for the optimal model during tensile test.

Elongation of the chain during the tensile loading can be easily seen in the Figure 4.6.

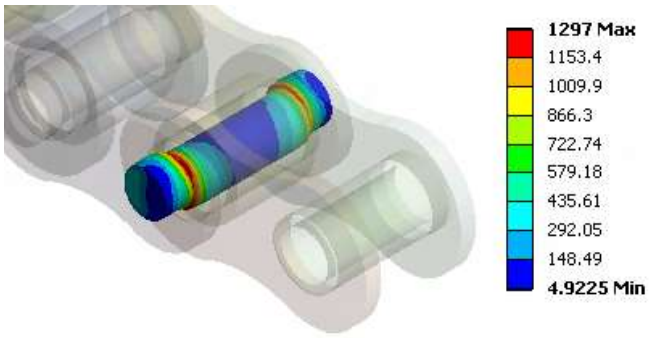

Figure 4.7: Stress variation over the most stressed member (MPa) for the optimal model during tensile test.

Maximum stress was observed over Pin, Figure 4.7 shows the equivalent von-Mises stress variation over the pin during its loading.

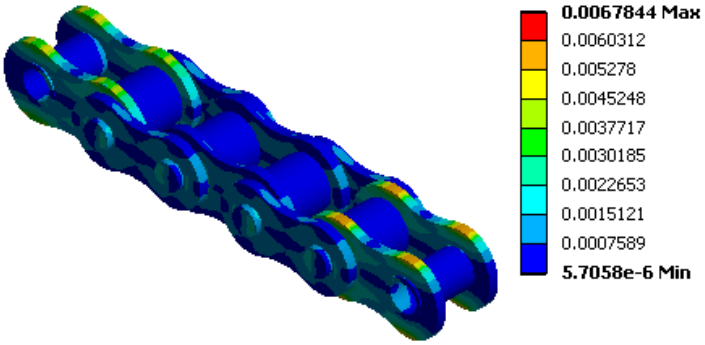

Figure 4.8: Strain variation over the chain for the optimal model during tensile test.

Figure 4.8 shows the strain variation over the entire chain component.

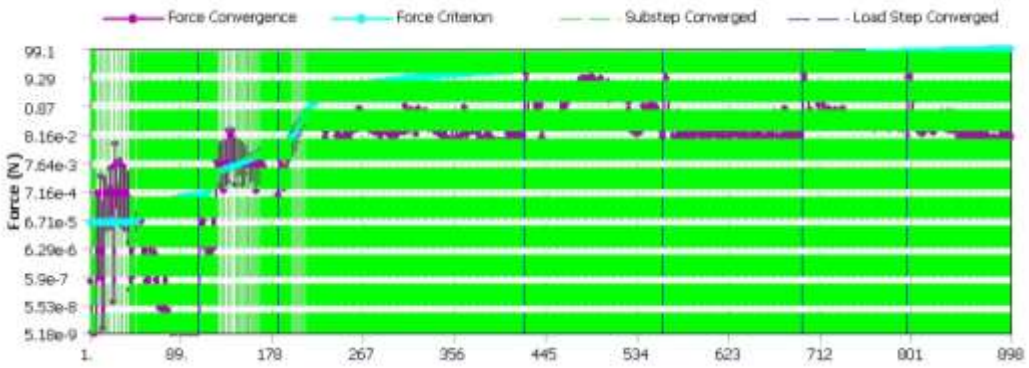

Figure 4.9: Force convergence graph of the solution for the optimal model during tensile test.

Force convergence of the solution is shown in Figure 4.9. It took 898 iterations to successfully solve the model.

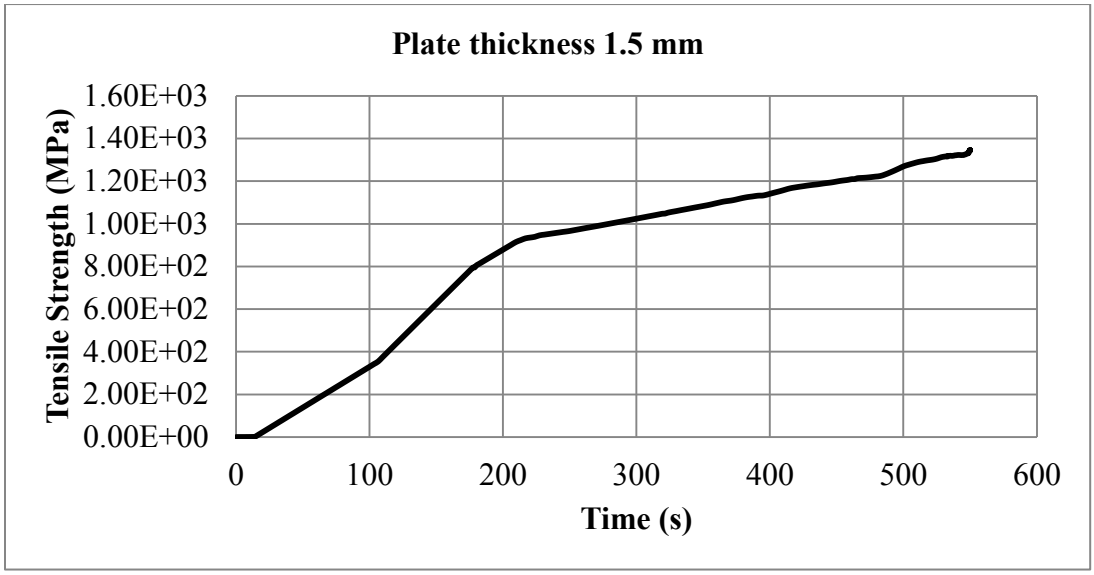

Figure 4.10: Stress history for the optimal model during tensile test.

Stress of 1306.2 MPa came at time 525.46 seconds. The curve in the Figure 4.10 shows the stress levels at the different time interval in the solution. At the end of first step when gravity was applied the stress value was found to be 2.76E-01 MPa. The stress value at the end of each step is shown in Figure 4.11 along with the load applied during the respective step.

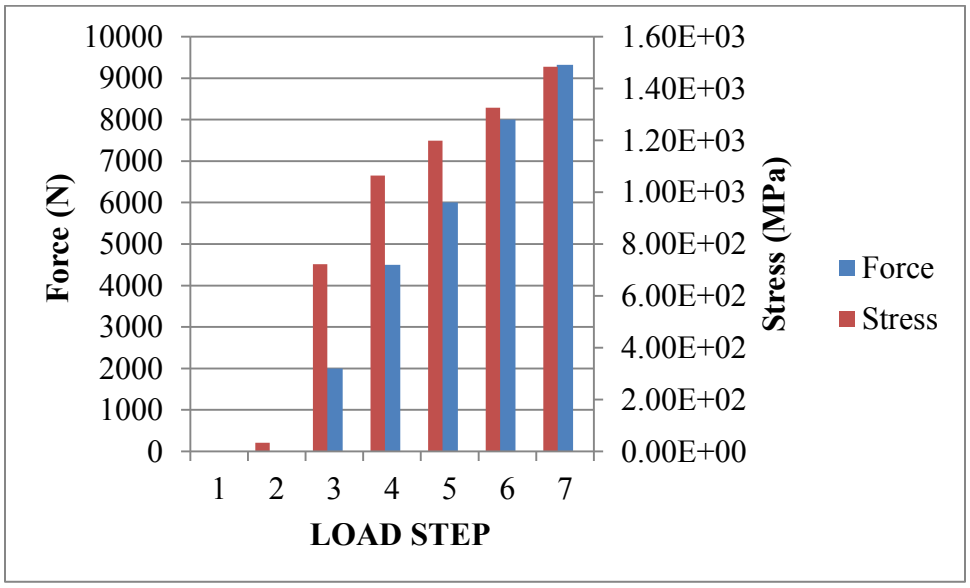

Figure 4.11: Stress (MPa) and Force (N) at the end of each load step for the optimal model during tensile test.

4.1.3 Model optimization for Chain Weight Reduction.

A model which can easily predict the tensile strength of the chain drive as discussed in Section 4.1.2 was successfully made, based on which it was optimized for the given dimensional tolerance. Initially, the plate thickness (shown as dimension d0:6 and d0:4 in Figure 3.6) whose value was 1.5 mm was varied in a given range of 1.5 mm to 1.2 mm (both inner plate and outer plate were kept at the same value). Tensile strength at each change was studied for reduction of 0.1 mm in the present value of 1.5 mm. All the other dimensions are held confidential with the company.

The distance between the inner plates and outer plates was kept constant. This constant distance got varied because of change in thickness. In order to keep both the plates at the set distance, pin and bush length was reduced. For every 0.1 mm reduction in the thickness, the pin length got reduced by four times and the bush length by two times. For our convenience, instead of any numerical value the original length of pin and bush are taken as d0:0 and ad4:2 respectively.

Starting with the thickness of 1.4 mm, the results are discussed below.

A. Thickness of plates reduced to 1.4 mm.

Thickness of inner plate as well as outer plate is reduced to 1.4 mm.

Pin length = PL-0.4 and Bush length = BL-0.2.

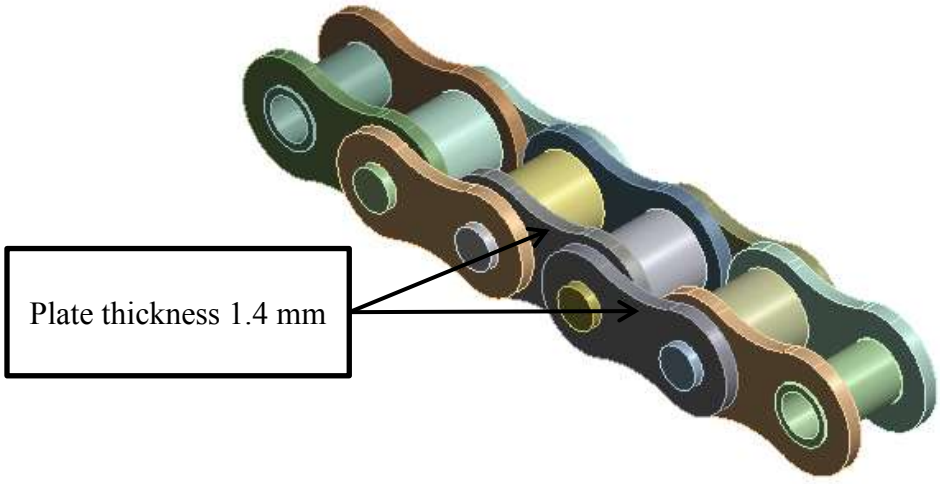

Figure 4.12: Model with 1.4 mm thick plates.

The model as shown in Figure 4.12 is solved for given boundary conditions. Tensile strength if found to be 1708 kgf. The stress variation over the entire model is shown in Figure 4.13.

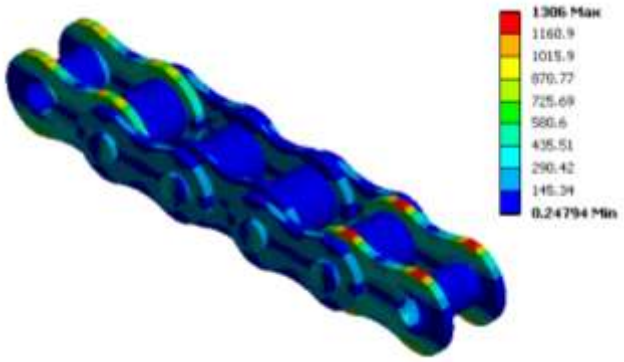

Figure 4.13: Stress variation over the chain (MPa) when the plate thickness is 1.4 mm for tensile test.

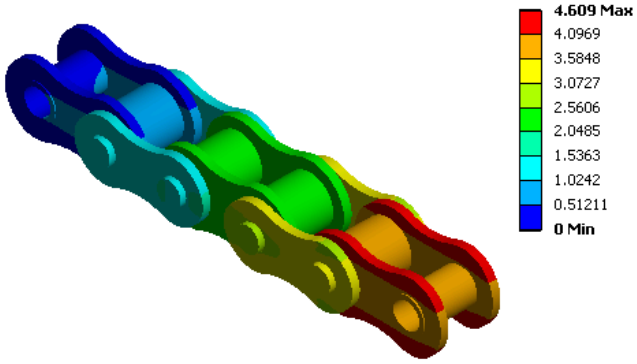

Figure 4.14: Deformation of the chain (mm) when the plate thickness is 1.4 mm for tensile test.

Elongation of the chain during the tensile loading can be easily seen in the Figure 4.14.

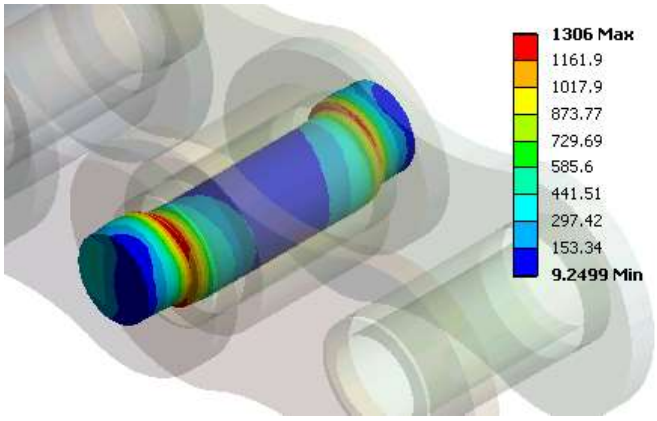

Figure 4.15: Stress variation over the most stressed member (MPa) when the plate thickness is 1.4 mm for tensile test.

Maximum stress was observed over Pin, Figure 4.15 shows the equivalent von-Mises stress variation over the pin during its loading.

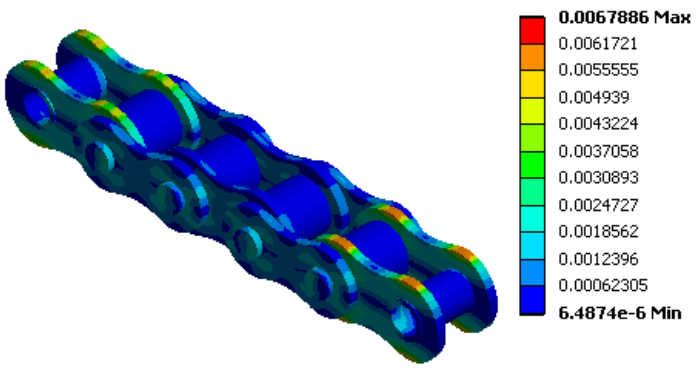

Figure 4.16: Strain variation over the chain when the plate thickness is 1.4 mm for tensile test.

Figure 4.16 shows the variation of strain over the model.

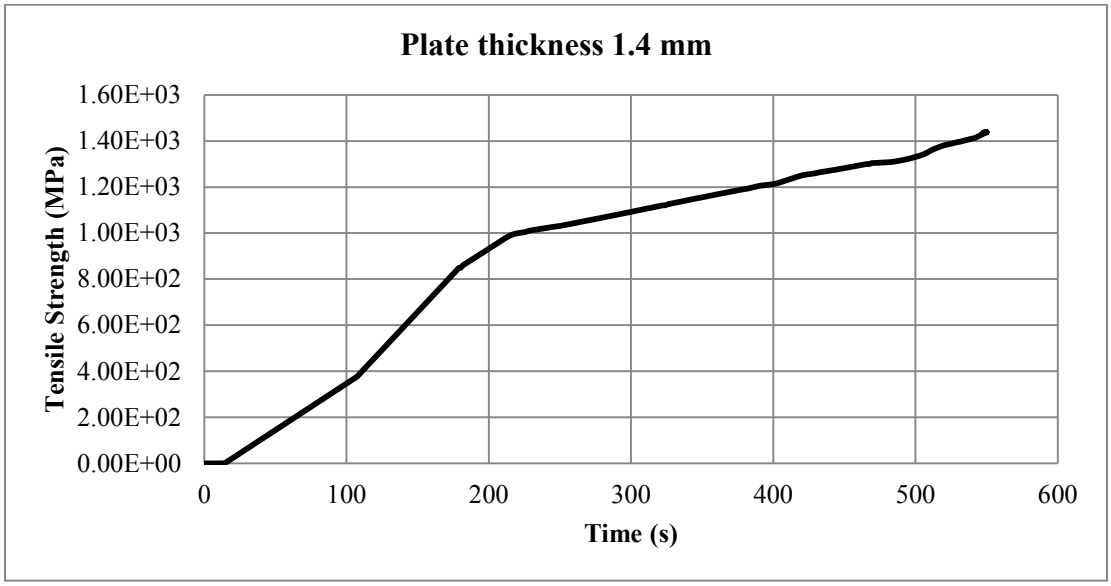

Figure 4.17: Stress history when the plate thickness is 1.4 mm for tensile test.

Stress of 1306 MPa came at time 476.76 seconds. The curve in the Figure 4.17 shows the stress levels at the different time interval in the solution. At the end of first step when gravity was applied the stress value was found to be 2.88E-01 MPa. The stress value at the end of each step is shown in Figure 4.18 along with the load applied during the respective step.

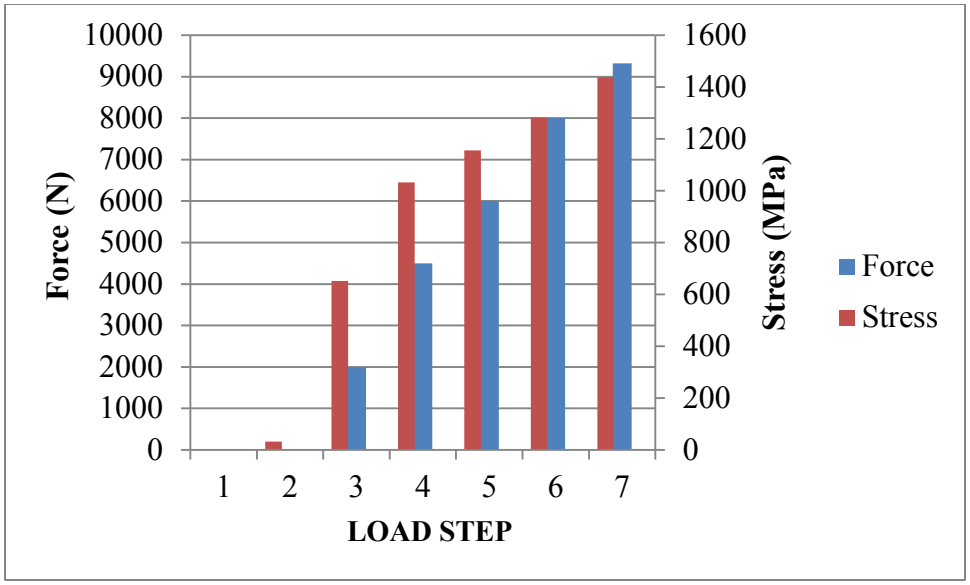

Figure 4.18: Stress (MPa) and Force (N) at the end of each load step when the plate thickness is 1.4 mm for tensile test.

B. Thickness of plates reduced to 1.3 mm.

Thickness of inner plate as well as outer plate is reduced to 1.3 mm.

Pin length = PL-0.8 and Bush length = BL-0.4.

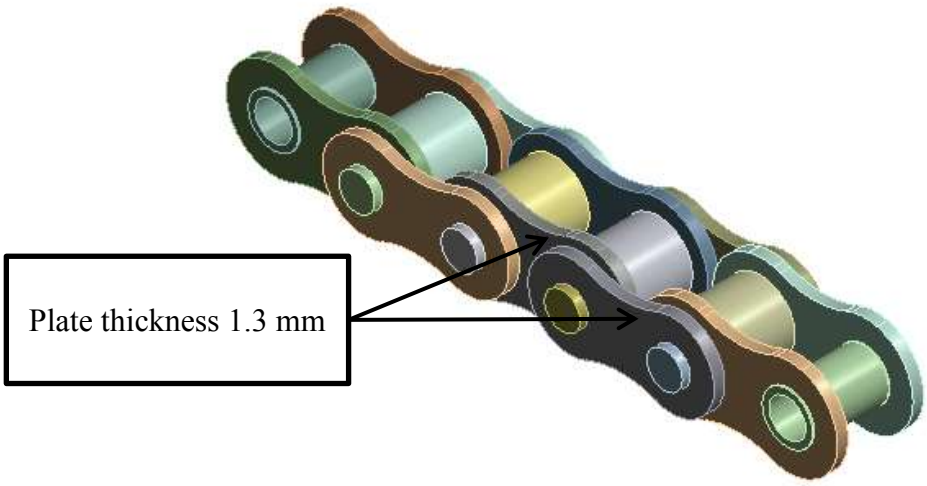

Figure 4.19: Model with 1.3 mm thick plates.

The model as shown in Figure 4.19 is solved for given boundary conditions. Tensile strength if found to be 1560 kgf. The stress variation over the entire model is shown in Figure 4.20.

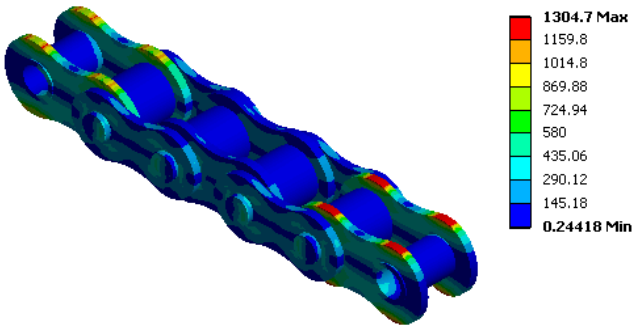

Figure 4.20: Stress variation over the chain (MPa) when the plate thickness is 1.3 mm for tensile test.

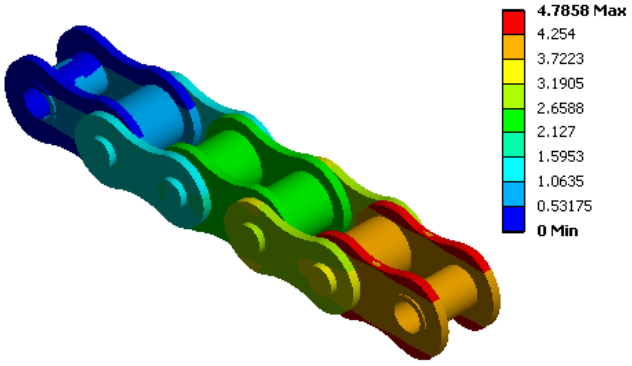

Figure 4.21: Deformation of the chain (mm) when the plate thickness is 1.3 mm for tensile test.

Elongation of the chain during the tensile loading can be easily seen in the Figure 4.21.

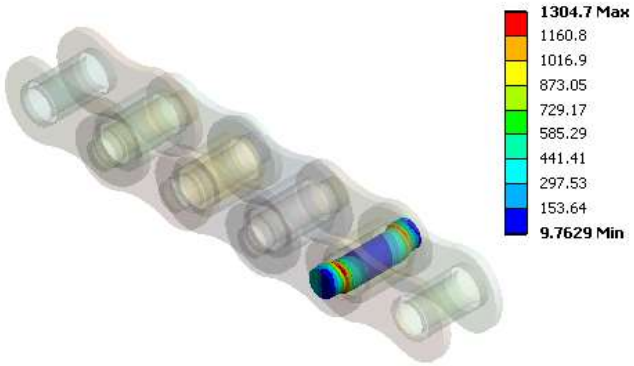

Figure 4.22: Stress variation over the most stressed member (MPa) when the plate thickness is 1.3 mm for tensile test.

Maximum stress was observed over Pin, Figure 4.22 shows the equivalent von-Mises stress variation over the pin during its loading.

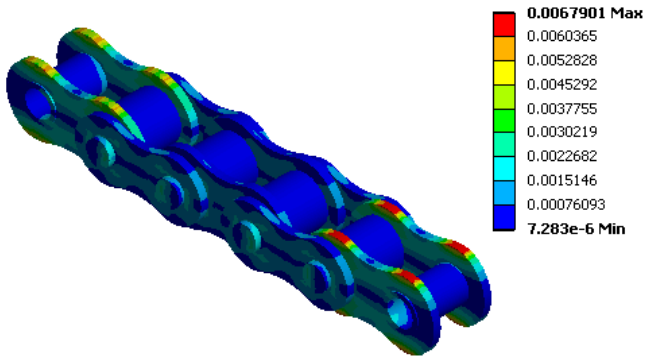

Figure 4.23: Strain variation over the chain when the plate thickness is 1.3 mm for tensile test.

Figure 4.23 shows the variation of strain over the model.

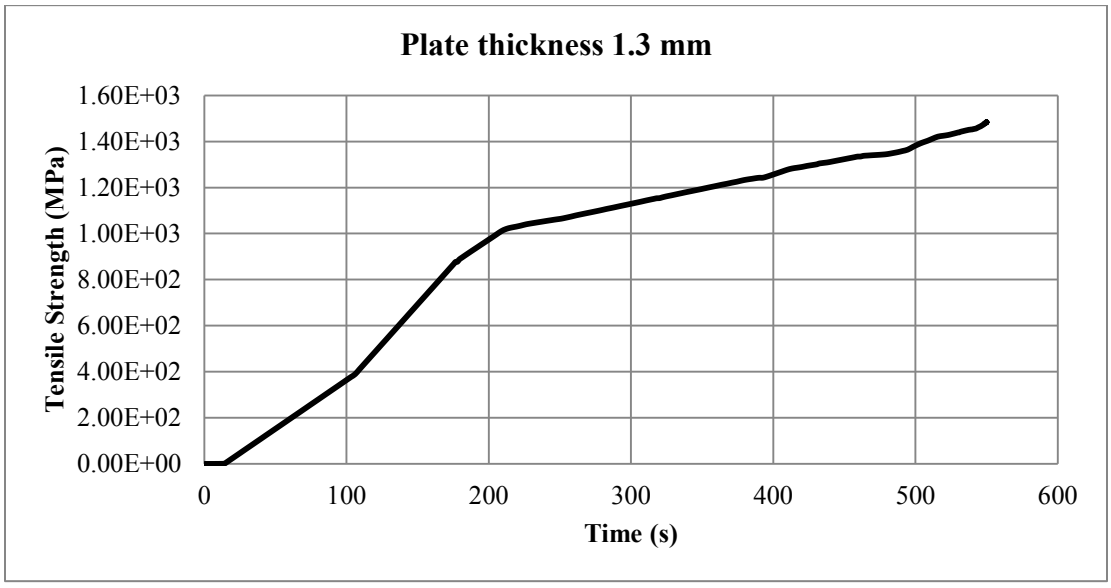

Figure 4.24: Stress history when the plate thickness is 1.3 mm for tensile test.

Stress of 1304.7 MPa came at time 432.59 seconds. The curve in the Figure 4.24 shows the stress levels at the different time interval in the solution. At the end of first step when gravity was applied the stress value was found to be 2.95E-01 MPa. The stress value at the end of each step is shown in Figure 4.25 along with the load applied during the respective step.

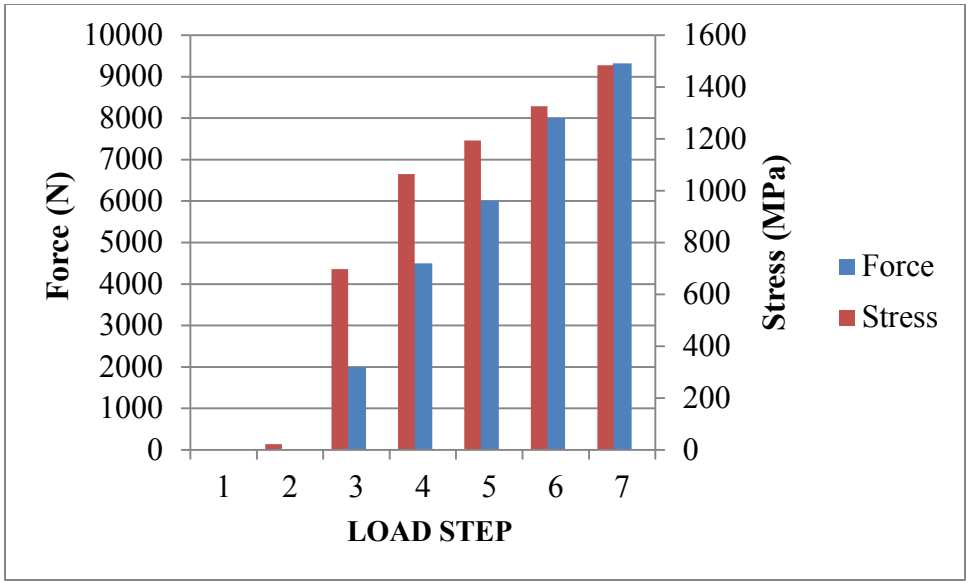

Figure 4.25: Stress (MPa) and Force (N) at the end of each load step when the plate thickness is 1.3 mm for tensile test.

C. Thickness of plates reduced to 1.2 mm.

Thickness of inner plate as well as outer plate is reduced to 1.2 mm.

Pin length = PL-1.2 and Bush length = BL-0.6.

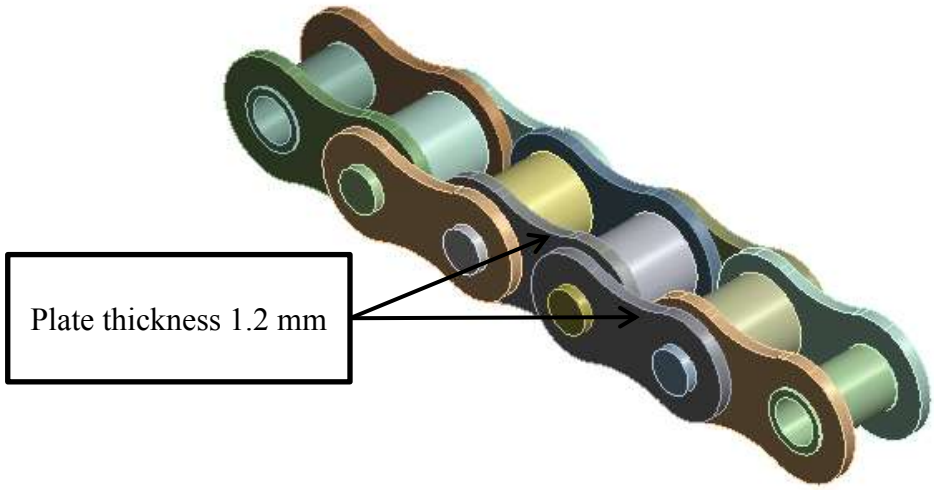

Figure 4.26: Model with 1.2 mm thick plates.

The model as shown in Figure 4.26 is solved for given boundary conditions. Tensile strength if found to be 1411 kgf. The stress variation over the entire model is shown in Figure 4.27.

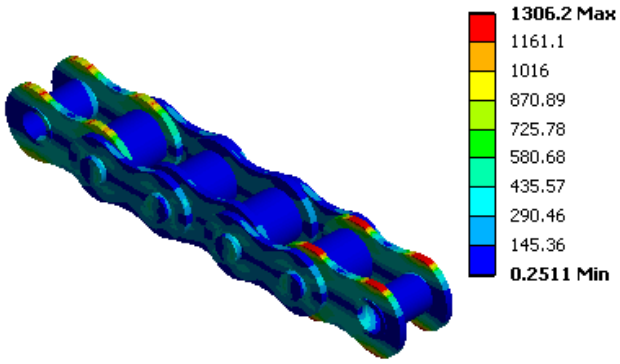

Figure 4.27: Stress variation over the chain (MPa) when the plate thickness is 1.2 mm for tensile test.

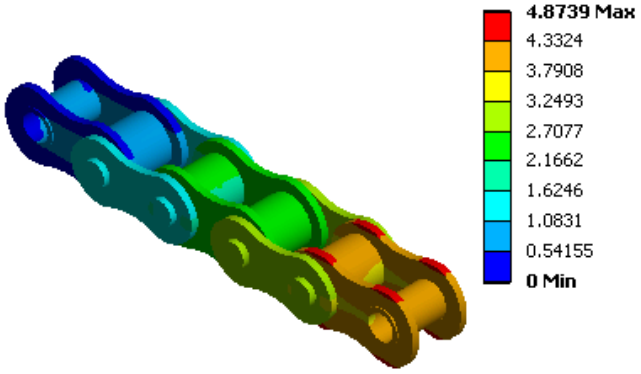

Figure 4.28: Deformation of the chain (mm) when the plate thickness is 1.2 mm for tensile test.

Elongation of the chain during the tensile loading can be easily seen in the Figure 4.28.

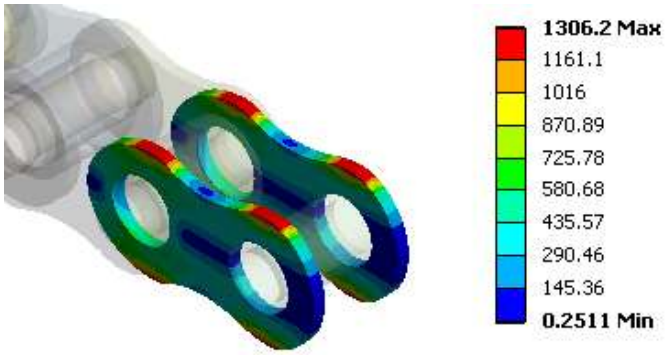

Figure 4.29: Stress variation over the most stressed member (MPa) when the plate thickness is 1.2 mm for tensile test.

Maximum stress was observed over Inner Plate, Figure 4.29 shows the equivalent von-Mises stress variation over the pin during its loading.

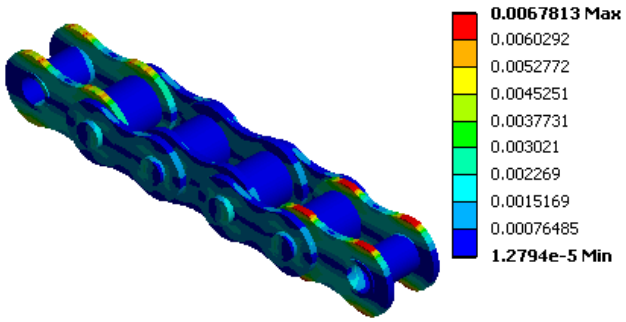

Figure 4.30: Strain variation over the chain when the plate thickness is 1.2 mm for tensile test.

Figure 4.30 shows the variation of strain over the model.

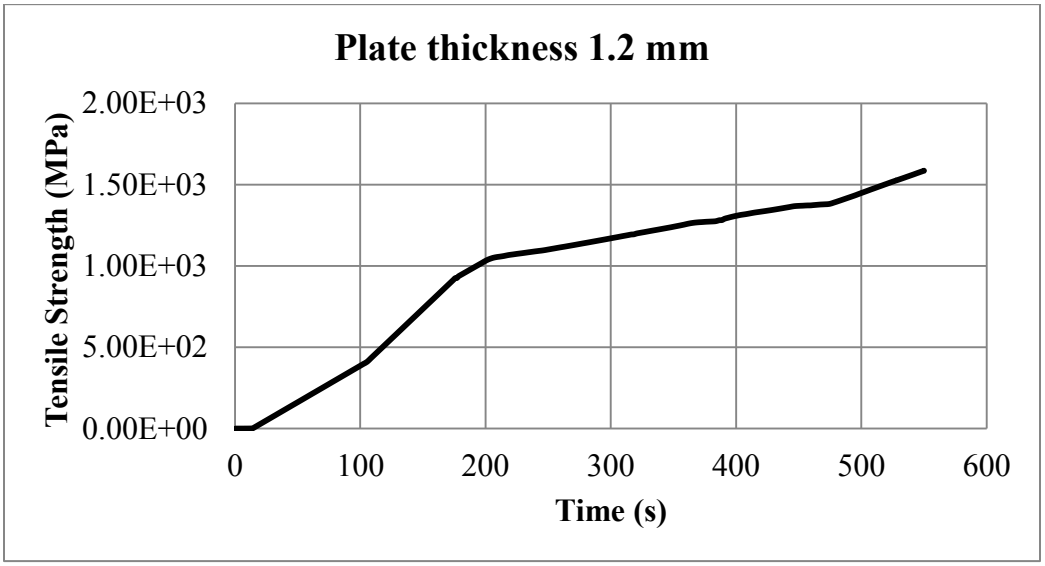

Figure 4.31: Stress history when the plate thickness is 1.2 mm for tensile test.

Stress of 1306.2 MPa came at time 396.04775 seconds. The curve in the Figure 4.31 shows the stress levels at the different time interval in the solution. At the end of first step when gravity was applied the stress value was found to be 0.30584 MPa. The stress value at the end of each step is shown in Figure 4.32 along with the load applied during the respective step.

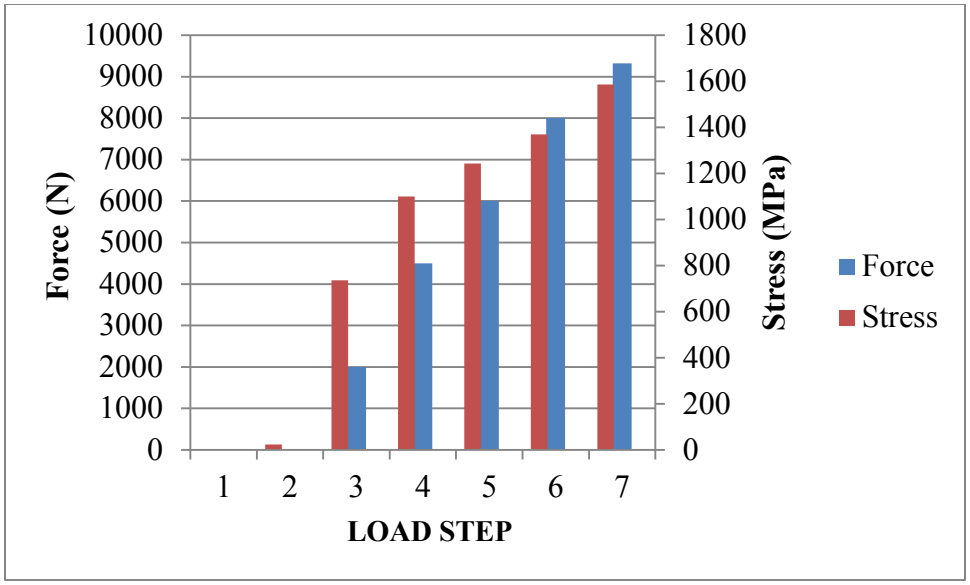

Figure 4.32: Stress (MPa) and Force (N) at the end of each load step when the plate thickness is 1.2 mm for tensile test.

D. Thickness of plates reduced to 1.2 mm with proposed design.

The chain manufacturer had also proposed a new design with a plate thickness of 1.2 mm. All the chain components were made with the new dimensions and the test was performed.

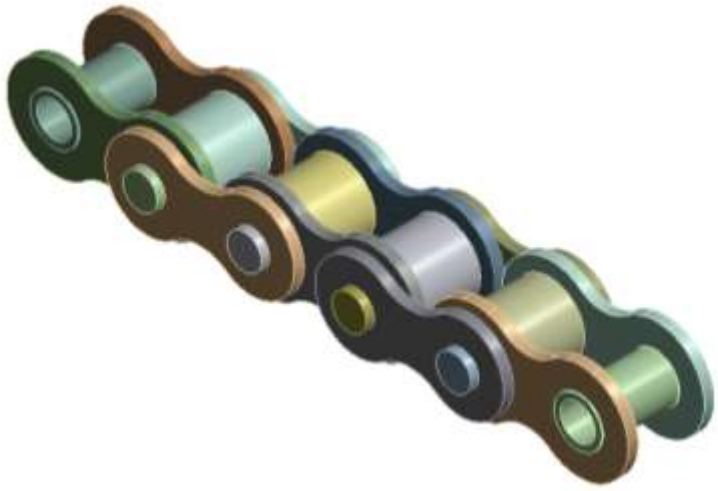

Figure 4.33: Model with 1.2 mm thick plates and proposed design.

The model as shown in Figure 4.33 is solved for given boundary conditions. Tensile strength if found to be 1371 kgf. The stress variation over the entire model is shown in Figure 4.34.

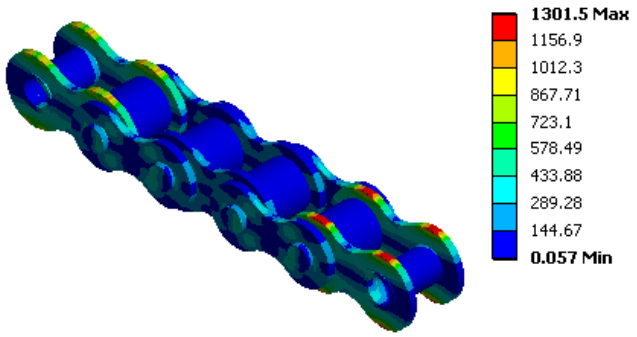

Figure 4.34: Stress variation over the chain (MPa) when the plate thickness is 1.2 mm with proposed design for tensile test.

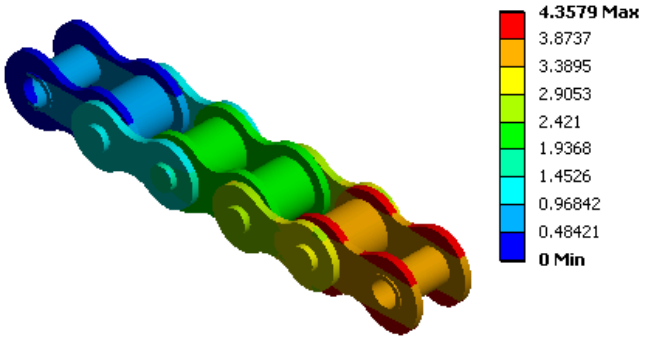

Figure 4.35: Deformation of the chain (mm) when the plate thickness is 1.2 mm with proposed design for tensile test.

Elongation of the chain during the tensile loading can be easily seen in the Figure 4.35.

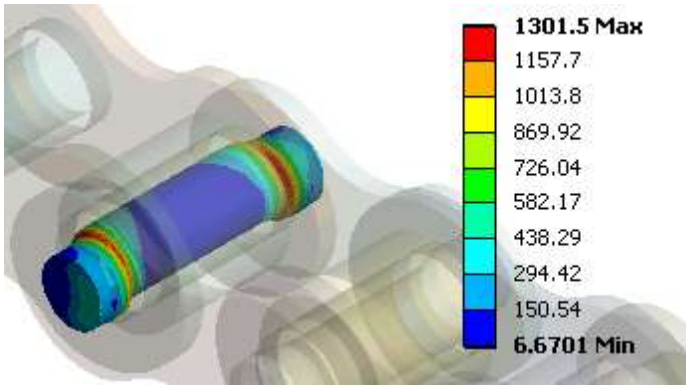

Figure 4.36: Stress variation over the most stressed member (MPa) when the plate thickness is 1.2 mm with proposed design for tensile test.

Maximum stress was observed over Pin, Figure 4.36 shows the equivalent von-Mises stress variation over the pin during its loading.

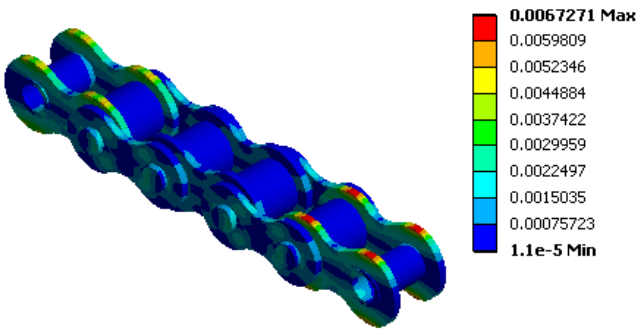

Figure 4.37: Strain variation over the chain when the plate thickness is 1.2 mm with proposed design for tensile test.

Figure 4.37 shows the variation of strain over the model.

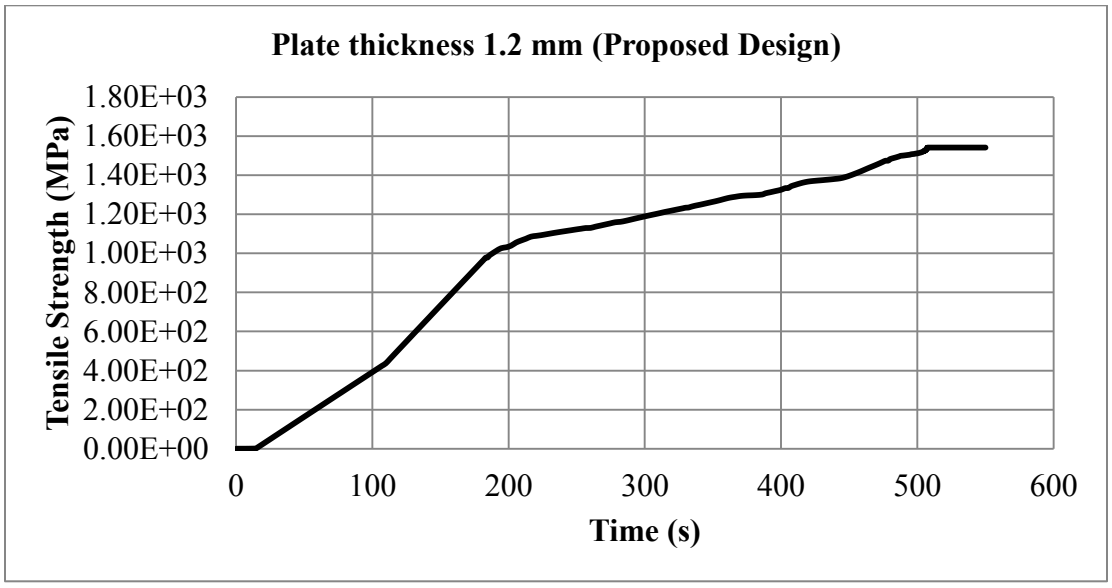

Figure 4.38: Stress history when the plate thickness is 1.2 mm with proposed design for tensile test.

Stress of 1301.5 MPa came at time 386.2375 seconds. The curve in the Figure 4.38 shows the stress levels at the different time interval in the solution. At the end of first step when gravity was applied the stress value was found to be 0.35891 MPa. The stress value at the end of each step is shown in Figure 4.39 along with the load applied during the respective step.

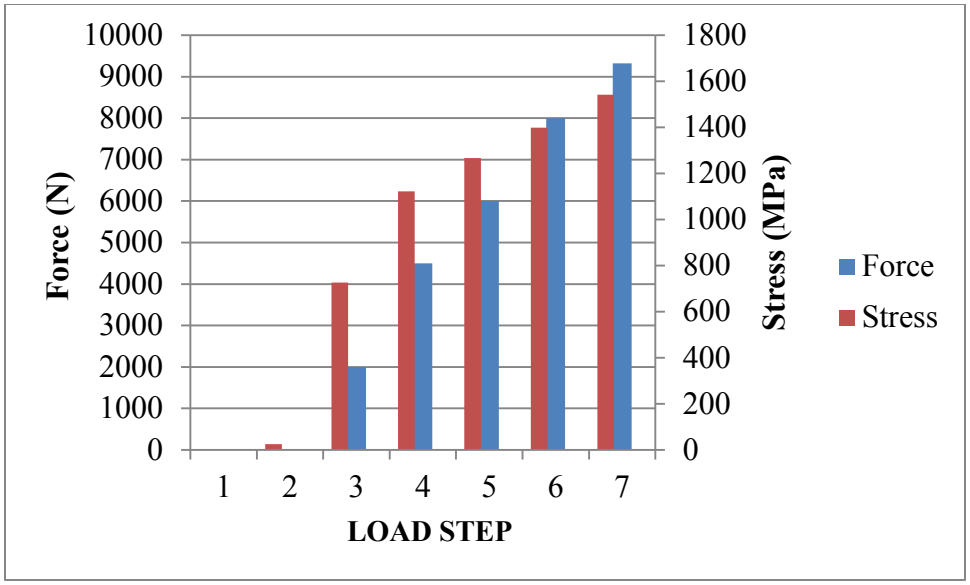

Figure 4.39: Stress (MPa) and Force (N) at the end of each load step when the plate thickness is 1.2 mm with proposed design for tensile test.

E. Increasing the strength of 1.2 mm thick chain with design change.

Proposed deign had a tensile strength of 1371 kgf. The strength of the chain with the proposed design can be further increased. In order to increase the strength of the chain a new dimensional change with a plate thickness of 1.2 mm was proposed and checked.

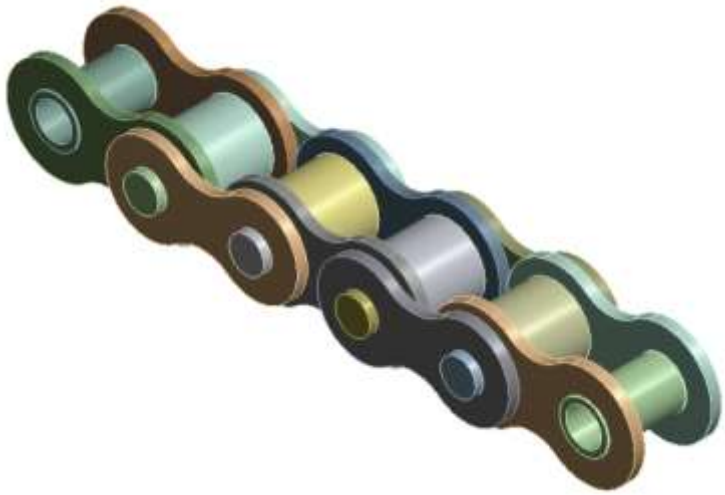

Figure 4.40: Model with 1.2 mm thick plates with design change.

The model as shown in Figure 4.40 is solved for given boundary conditions. Tensile strength if found to be 1480 kgf. The stress variation over the entire model is shown in Figure 4.41.

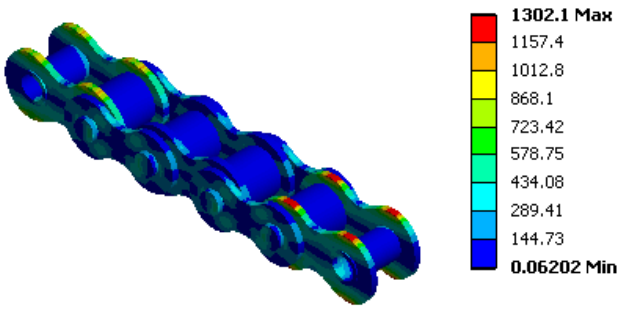

Figure 4.41: Stress variation over the chain (MPa) when the plate thickness is 1.2 mm with design change for tensile test.

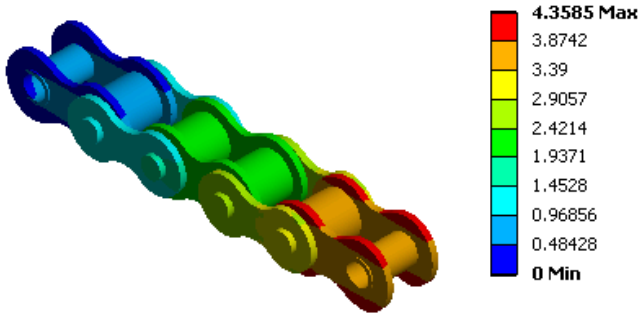

Figure 4.42: Deformation of the chain (mm) when the plate thickness is 1.2 mm with design change for tensile test.

Elongation of the chain during the tensile loading can be easily seen in the Figure 4.42.

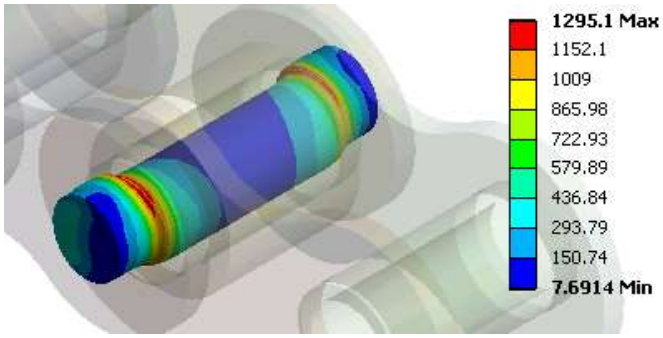

Figure 4.43: Stress variation over the most stressed member (MPa) when the plate thickness is 1.2 mm with design change for tensile test.

Maximum stress was observed over Pin, Figure 4.43 shows the equivalent von-Mises stress variation over the pin during its loading.

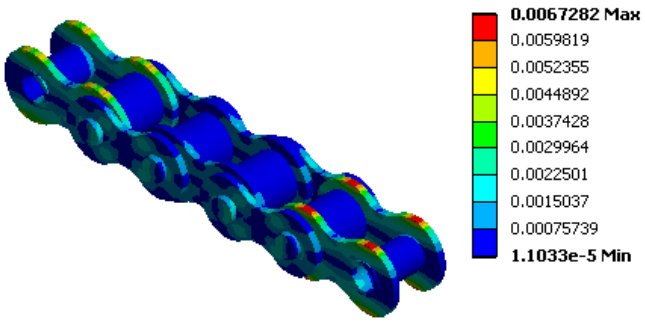

Figure 4.44: Strain variation over the chain when the plate thickness is 1.2 mm with design change for tensile test.

Figure 4.44 shows the variation of strain over the model.

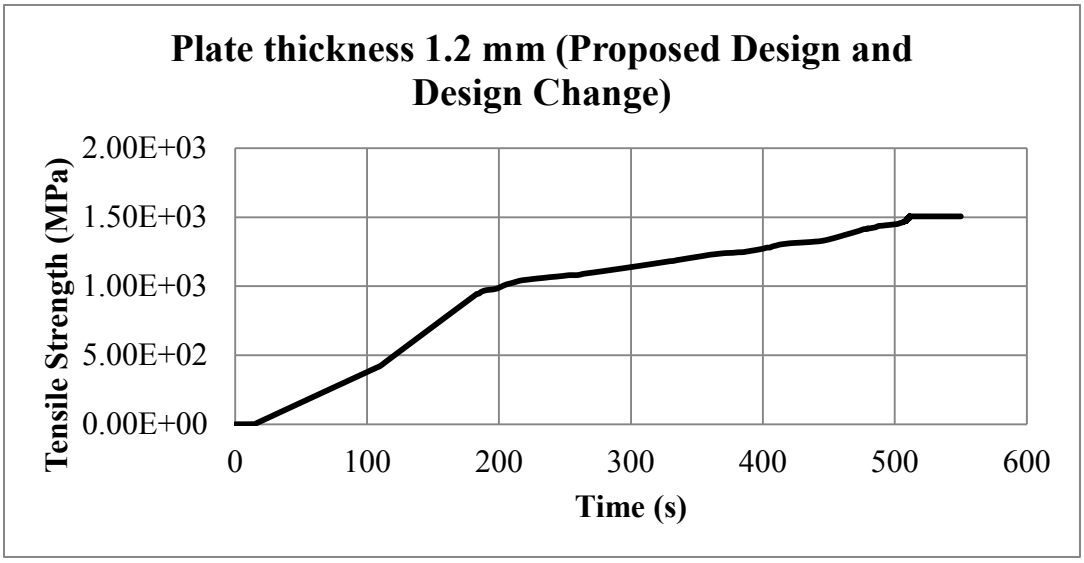

Figure 4.45: Stress history when the plate thickness is 1.2 mm with design change for tensile test.

Stress of 1302.1 MPa came at time 412.97 seconds. The curve in the Figure 4.45 shows the stress levels at the different time interval in the solution. At the end of first step when gravity was applied the stress value was found to be 0.35891 MPa. The stress value at the end of each step is shown in Figure 4.46 along with the load applied during the respective step.

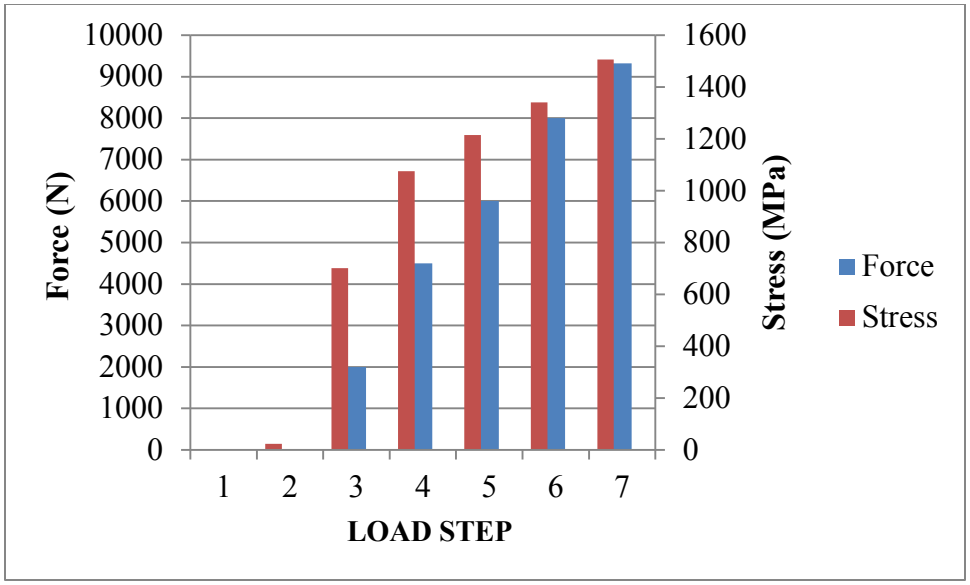

Figure 4.46: Stress (MPa) and Force (N) at the end of each load step when the plate thickness is 1.2 mm with design change for tensile test.

4.2 Fatigue Test

4.2.1 Model

As discussed earlier in section 3.7, a structural analysis is needed to complete the fatigue analysis, a transient structural analysis is done on the optimum model developed in section 3.5 of tensile test. Loading and boundary conditions developed as discussed in section 3.6. The load is applied as shown in Table 4.2.

Table 4.2: Load Step Details (Fatigue Test).

Time (s)	Force (N)	Gravity (mm/s^2)
0	0	0
10	0	9806.6
20	4	9806.6
100	190	9806.6
120	572	9806.6
140	954	9806.6
200	2100	9806.6

Maximum von-Mises stress on the model was found to be 491.92 MPa for the load of 420 kgf (shown in Figure 4.47) and elongation of 0.46712 mm was observed (shown in **Figure 4.48**).

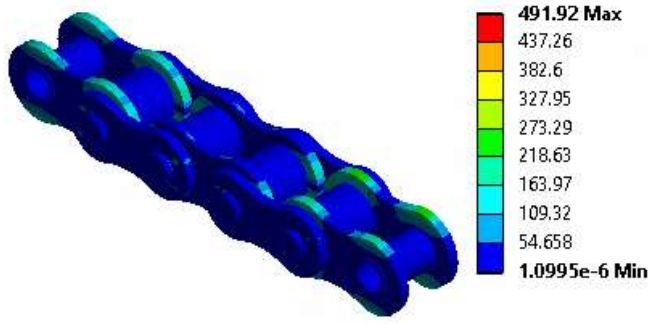

Figure 4.47: Stress variation over the chain (MPa) for fatigue test.

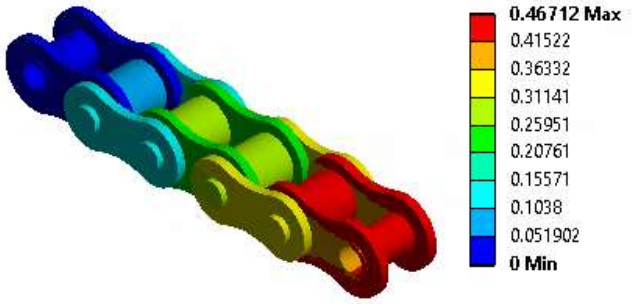

Figure 4.48: Deformation of the chain (mm) for fatigue test.

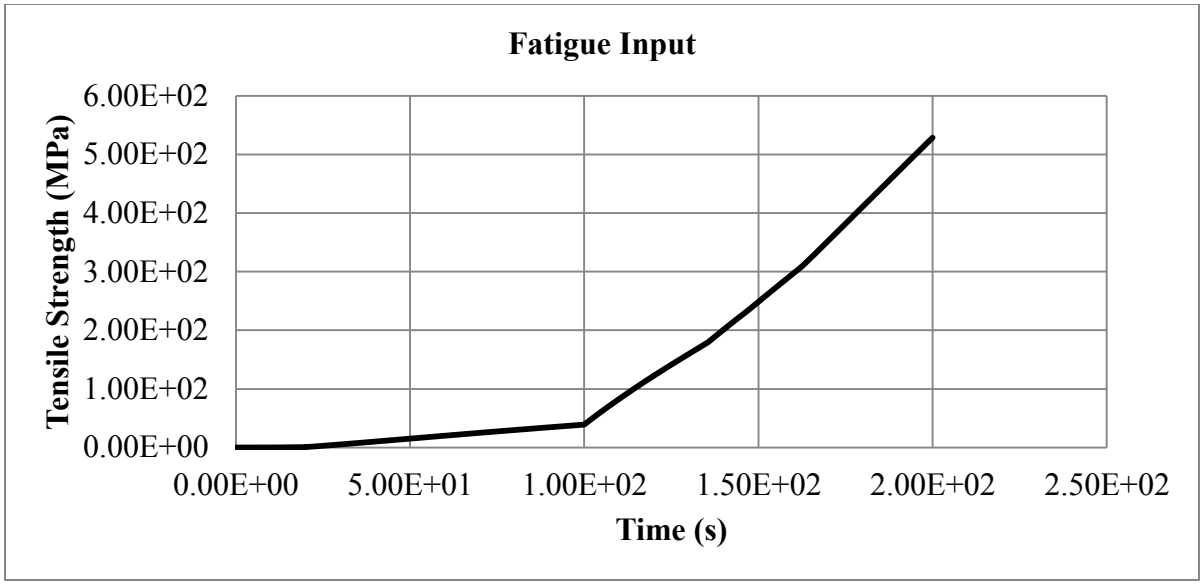

Figure 4.49: Stress history for fatigue test.

Figure 4.49 shows the stress variation over the chain with respect to the time. This model was further used to do the fatigue analysis.

4.2.2 Results

Desired life of the chain was 500000 cycles (for raw stage) and the simulation predicted the life of the chain to be 508825 cycles (shown in Figure 4.50).

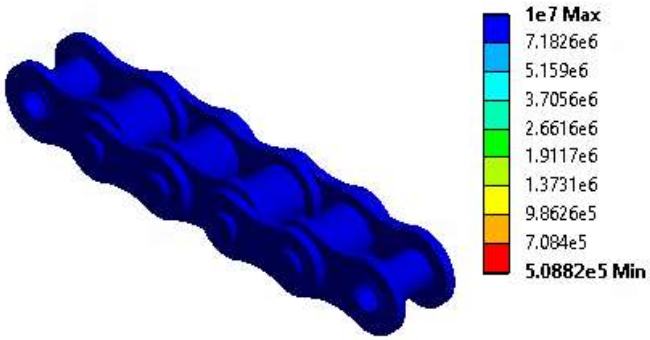

Figure 4.50: Fatigue Life of Chain (cycles).

Fatigue tool can predict two more quantities, the Damage and Safety Factor. In order to predict these quantities, it requires an additional input of the desired Design Life which is taken as 500000 cycles. Fatigue damage is design life divide by available life and Safety factor is a contour plot of the factor of safety (FS) with respect to a fatigue failure at a given design life. The maximum FS reported is 15.

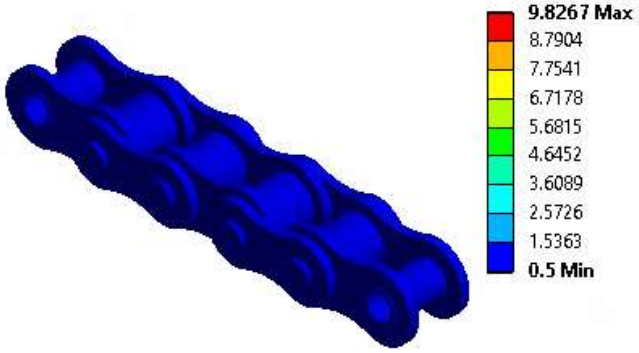

Figure 4.51: Fatigue Damage to the chain.

Figure 4.51 and Figure 4.52 shows the damage to the chain and safety factor of the chain. The calculated damage is 9.8267 and safety factor is 0.92799 .

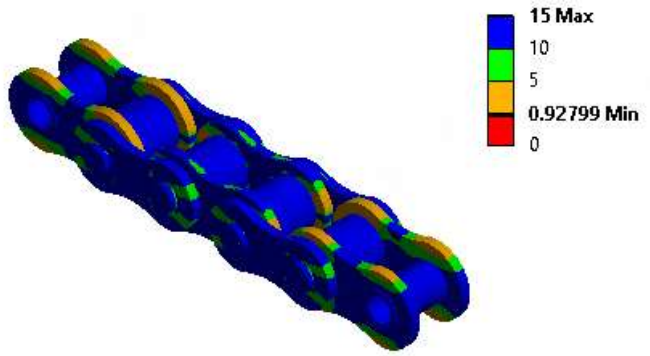

Figure 4.52: Safety Factor of the chain.

4.3 Endurance Test

Model for the endurance test was already discussed in section 3.7. Coarse mesh was selected so as to compensate the computer requirements which generated 424698 numbers of nodes and 84426 elements. During meshing, it was also checked that the gap between the rollers and sprocket is present as shown in Figure 4.53

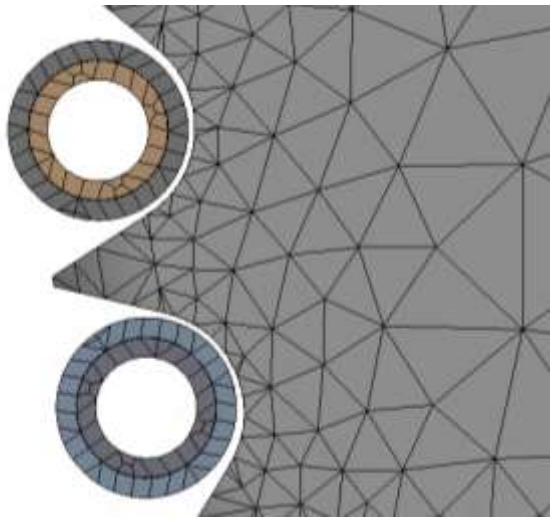

Figure 4.53: Initial gap in between the rollers and sprocket.

This gap was necessary so as to properly initiate the frictional contacts in between the rollers surrounding the sprocket. The assembly could have been modeled with the surface of roller touching the sprocket, but at the time of meshing, the elements would penetrate each other which would lead to unconvergence of the solution. Hence each roller overlapping both the sprockets was properly checked after the mesh.

First step in the analysis was to initiate the frictional contacts which had initially gap in between them. Small sprocket was kept fixed with only rotational degree of freedom and the big sprocket was moved axially to close this gap and initiate the contact in between the rollers and the sprocket. After completion of this load step, rotation to the joint connecting the small sprocket was given (shown in Figure 4.54). Load step details are shown in Table 4.3

Table 4.3: Load step details (Endurance Test).

Time (s)	Displacement (mm)	Rotation (Degree)
50	5	0
100	5	100

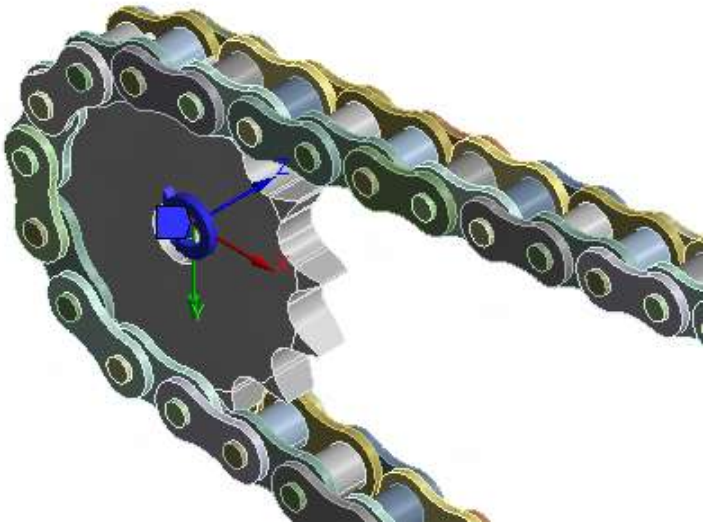

Figure 4.54: Joint load 'Rotation' given to sprocket.

Convergence Problem:-

The model took time to prepare on account of large number of linear and non-linear contacts. Huge amount of physical memory was needed to run the model even with coarse mesh. A new convergence criterion, Displacement Convergence was added to the existing Force Convergence because of the Joints included in this model. Force always converged easily for this model but displacement convergence was an issue. Initially the model got easily converged for a few seconds, but as the sprocket came in contact with the roller, the displacement convergence moved far away from the displacement criterion.

The convergence graph is shown in Figure 4.55 in which a sudden rise is seen in the displacement convergence line as a result of bodies including frictional contact coming in contact with each other. The solution got successfully solved till a time step of 6.38 seconds after which it failed to converge undergoing many bisections.

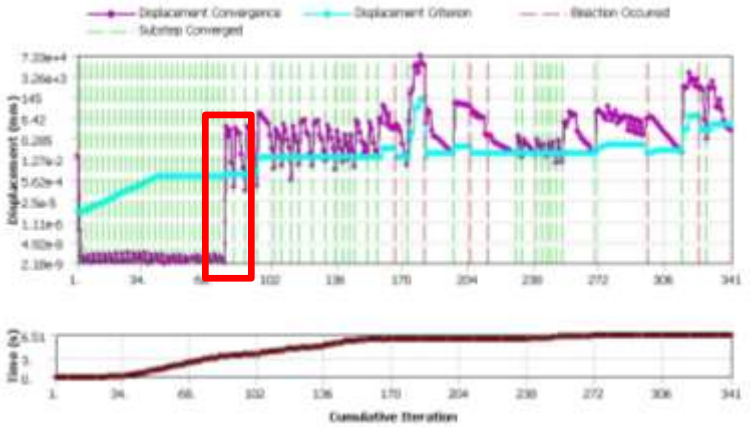

Figure 4.55: Partially converged solution.

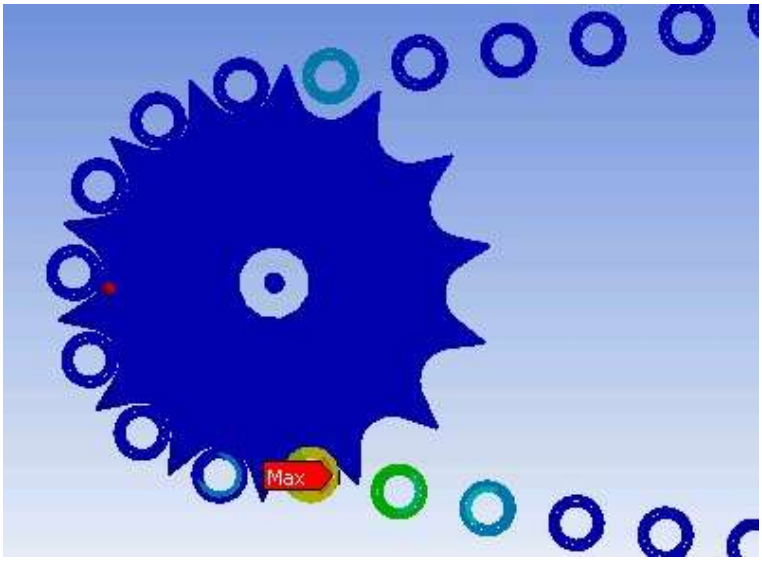

Figure 4.56: Displacement results of the partially solved solution.

The displacement of the unsolved solution is shown in the Figure 4.56 in which the body with the maximum deformation undergoes a sudden change in its position.

This uneven behaviour of the body was due to improper time stepping which was corrected and model was send to simulation. The graph in Figure 4.57 is the displacement convergence which shows that the sudden rise in the simulation has been corrected to some extend and the solution is converging and no bisections have occurred.

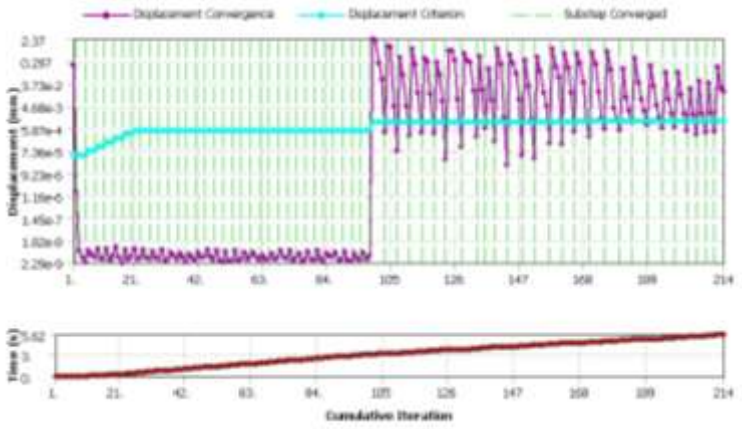

Figure 4.57: Displacement convergence graph of the model undergoing simulation.

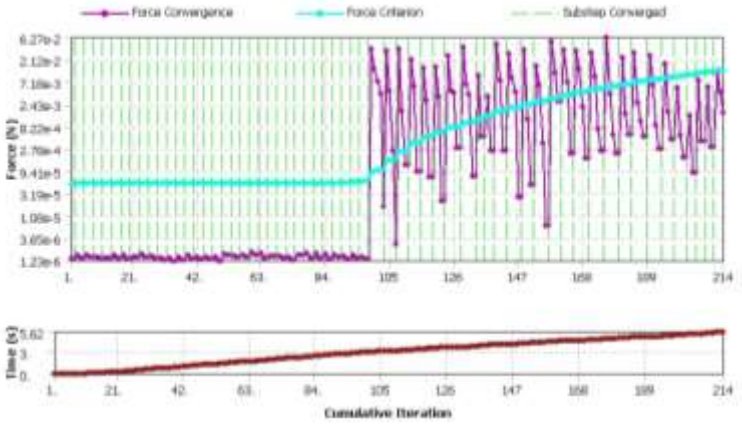

Figure 4.58: Force convergence graph of the model undergoing simulation.

Force convergence of the model can be successfully studied with the help of graph shown in Figure 4.58 and it can be seen that the model is undergoing convergence and at the end the force convergence line is coming under the force criterion.

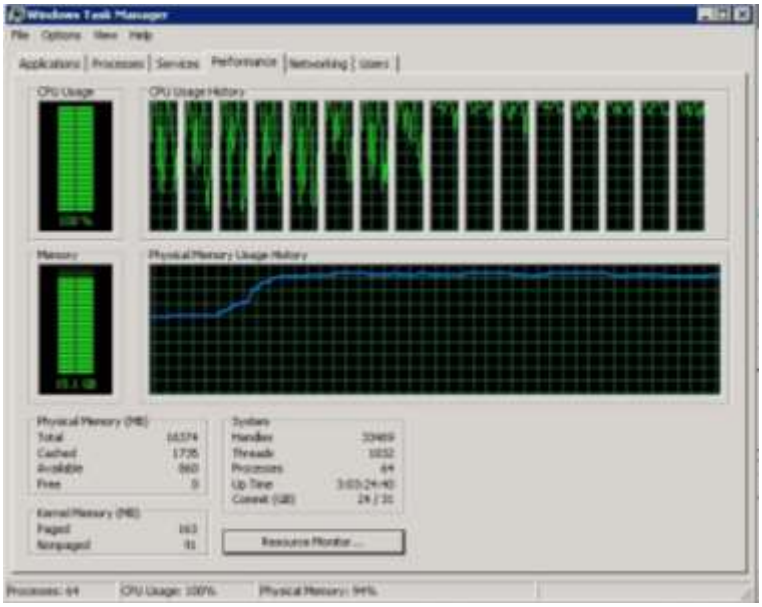

Figure 4.59: Computer Usage during the simulation.

Computer used to perform the simulation was a 16 core (2.26 GHz each core), 16 GB RAM and 750 GB Hard Disk windows based Workstation. During the simulation, 100 % CPU utilization was done on 15.1 GB of memory which can be seen from the Figure 4.59. The undergoing simulation is expected to converge fully with the changes made in it. It may be possible that the solution does not converge, the remedies are discussed in the next chapter.

Chapter 5 CONCLUSION AND SCOPE OF FUTURE WORK

5.1 Conclusion

Based on present work of developing model for tensile test, fatigue test and endurance test and results obtained, the following conclusions are drawn:

1. Seamless bush is found superior over the seamed bush and can be used in the new chain manufacturing.
2. Contact non-linearity is successfully simulated with the help of frictional contact. Material data for the plastic region had been given as input to include the material non-linearity and the strain variation over the model can be successfully observed.
3. Based on the proposed dimensions, a new model has been proposed with high tensile strength than the proposed one.
4. A graphical visualization of the stresses developed on the body and chain elongation is made and the most stressed body is predicted. Fatigue life, factor of safety and fatigue damage is correctly predicted with the help of fatigue model developed.
5. Tensile test and fatigue test can be done easily and any load change can be easily incorporated in the test as compared to the actual testing which required a high amount of lead time, changes in dies, jigs and fixtures. Hence, geometry and material change for all the models can be successfully evaluated without manufacturing the chain.
6. Endurance model has been tried to establish but failed because of convergence issue.
7. Use of parametric model removed the hectic task of creating new model for every change in a particular dimension. Any dimensional change can be easily included within no time and use of relations in between two bodies gave automatic regeneration of second body whenever the dimension of first body is changed.

5.2 Scope of future work

Use of finite element method has helped to develop successfully the models which can predict the tensile strength and fatigue life. There are a lot of new elements being developed and a number of new methods which leave the future scope unbounded. Scope of future work is being discussed below.

1. For tensile testing, the fracture can also be graphically shown with the help of fracture data being specified along with the material data.
2. Model Order reduction software's are available which can reduce the model to a good extent and reduce the computational resources need and time required for the simulation.
3. If model reduction is not possible, then cloud computing can be done and two or more computers can be used parallel to solve the model.
4. FEA packages has capability to calculate the damage matrix, rainflow matrix, hysteresis and fatigue sensitivity based on the proper fatigue material data.
5. Endurance model failed to converge and below are some of the methods which can help the model converge.
    a. Mesh the model with higher relevance.
    b. Decrease the time stepping, divide displacement and rotation into more number of steps starting with a negligible amount of load and increase the total time.
    c. During the first sub-step in which the sprocket is displaced, lock all the joints which can help in locking the bodies when they come in contact with each other and help in decreasing the error in between the displacement convergence and displacement criterion.
    d. Another approach can be such that fix all the bodies other than those overlapping the sprocket, move the sprocket such that it comes under contact with these bodies. Once these contacts are satisfied give further displacement to the sprocket unlocking few number of bides in each step.

REFERENCES

[1] M M Woolfson and G J Pert, An Introduction to Computer Simulation.: Oxford University Press, 1999.

[2] O C Zienkiewicz and R L Taylor, The Finite Element Method. London: McGraw-Hill Co., 1989.

[3] http://www.chain-guide.com

[4] J C Conwell, An Examination of Transient Forces in Roller Chain Drives. Ph.D. Dissertation: Vanderbilt University, Nashville, TN, 1989.

[5] N C Bremer, "Heavy Duty Chain Drives for Marine Propulsion Service," Trans. ASME, vol. 69, pp. 441-452, 1947.

[6] W K Staments, "Dynamic Loading of Chain Drives," Trans. ASME, pp. 655-665, July 1951.

[7] R C Binder, Mechanics of the Roller Chain Drive. Englewood Cliffs, New Jersey, USA: Prentice-Hall, 1956.

[8] R A Morrison, "Polygonal Action in Chain Drives," Machine Design, vol. 24, pp. 155-159, 1952.

[9] S Mahalingam, "Polygonal action in chain drives," Journal of the Franklin Institute, vol. 265, no. 1, pp. 23-28, January 1858.

[10] M Okoshi and K Uehara, "Study on the Uneveness of Transmission Roller Chains," Journal of the Japan Society of Precision Engineering, vol. 25, no. 9, pp. 425-431, 1959.

[11] G Bouillon and G V Tordion, "On Polygonal Action in Roller Chain Drives," Journal of Engineering for Industry, ASME Transactions, vol. 87, pp. 243–250, 1965.

[12] G K Ryabov, "Inertial Effects of Impact Loading in Chain Drives," Russian Engineering Journal, vol. 48, no. 8, pp. 17-19, 1968.

[13] M Chew, "Inertia Effects of a Roller-Chain on Impact Intensity," Journal of Mechanisms, Transmissions, and Automation in Design, vol. 107, pp. 123–130, 1985.

[14] E I Radzimovsky, "Eliminating Pulsations in Chain Drives," Product Engineering, vol. 26, pp. 153-157, 1955.

[15] S R Turnbull and J N Fawcett, "An Approximate Kinematic Analysis of the Roller Chain

Drive," Proceedings of the Fourth World Congress on Theory of Machines and Mechanisms, pp. 907-911, 1975.

[16] K M Marshek, "On the Analyses of Sprocket Load Distribution," Mechanism and Machine Theory, vol. 14, pp. 135-139, 1978.

[17] K M Marshek and M O Ross, "Four-Square Sprocket Test Machine," Mechanism and Machine Theory, vol. 17, no. 5, pp. 321-326, 1982.

[18] K M Marshek and M Naji, "Analysis of Sprocket Load Distribution," Mechanism and Machine Theory, vol. 18, no. 5, pp. 349-356, 1983a.

[19] K M Marshek and M Naji, "Experimental Determination of the Roller Chain Load Distribution," Trans. ASME J. Mechanisms, Transmissions and Automation in Design, vol. 105, pp. 331-338, 1983b.

[20] B H Eldiwany and K M Marshek, "Experimental Load Distributions for Double Pitch Steel Roller Chains on Steel Sprockets," Mechanism and Machine Theory, vol. 19, no. 6, pp. 449-457, 1984.

[21] C K Chen and F Freudenstein, "Toward a More Exact Kinematics of Roller Chain Drives," Trans. of the ASME. Mechanisms. Transmissions and Automation in Design, vol. 110, no. 3, pp. 269-275, 1988.

[22] N C Veikos and F Freudenstein, "On the Dynamic Analysis of Roller Chain Drives :Part 1-Theory," Mechanism Design and Synthesis, vol. 46, pp. 431-438, 1992a.

[23] N C Veikos and F Freudenstein, "On the Dynamic Analysis of Roller Chain Drives: Part 2," Mechanism Design and Synthesis, vol. 46, pp. 439-450, 1992b.

[24] K W Wang, "On the Stability of Chain Drive Systems Under Periodic Sprocket Oscillations," Vibration and Acoustics, vol. 114, pp. 119-126, 1992.

[25] K W Wang and et al, "On the Impact Intensity of Vibrating Axially Moving Roller Chains," Vibration and Acoustics, vol. 114, pp. 397-403, 1992.

[26] M S Kim and G E Johnson, "Mechanics of Roller Chain-Sprocket Contact," MEAM Technical Report Number 92-06, 1992a.

[27] M S Kim and G E Johnson, "A General Multi-Body Dynamic Model to Predict the Behavior of Roller Chain Drives at Moderate and High Speeds," in MEAM Technical Report Number 92-07, 1992b.

[28] W Choi and G E Johnson, "Vibration of Roller Chain Drives at Low. Medium and High Operating Speeds," Vibration of Mechanical Systems and the History of Mechanical Design,ASME, vol. 63, pp. 29–40, 1992a.

[29] W Choi and G E Johnson, "Transverse Vibrations of a Roller Chain Drive with Tensioner," Vibrations of Mechanical Systems and the History of Mechanical Design, ASME, vol. 63, pp. 19-28, 1992b.

[30] Sabry A El-Shakery, "Kinematic analysis of combined roller-chain and planar mechanisms," Mechanism and machine theory, vol. 27, no. 6, pp. 715-728, 1992.

[31] Yeongching Lin, Sheng-Jiaw Hwang, Pete Pandolfi, Sam McDonald, and Jason Weidman, "The Dynamic Analysis of an Automotive Timing Chain System," vol. Ph.D. dissertation, 1993.

[32] K H Low, "Computer-aided selection of roller chain drives," Computers & Structures, vol. 55, no. 5, pp. 925-936, June 1995.

[33] James C Conwell and G E Johnson , "Design, Construction and Instrumentation of a Machince to Measure Tension and Impact Forces in Roller Chain Drives," Mechanism and Machine Theory, vol. 31, May 1995.

[34] James C Conwell and G E Johnson , "Experimental investigation of link tension and roller-sprocket impact in roller chain drives," Mechanism and Machine Theory, vol. 31, no. 4, pp. 533-544, May 1995.

[35] H Zheng et al., "Efficient modelling and prediction of meshing noise from chain drives," Journal of Sound and Vibration, vol. 245, no. 1, pp. 133-150, 2001.

[36] Kuen-Bao Sheu, Chih-Wei Chien, Shen-Tarng Chiou, and Ta-Shi Lai, "Kinetostatic analysis of a roller drive," Mechanism and Machine Theory, vol. 39, no. 8, pp. 819-837, August 2004.

[37] Stuart Burgess and Chris Lodge, "Optimisation of the chain drive system on sports motorcycles," Sports Engineering, ISEA, vol. 7, pp. 65-73, 2004.

[38] Sine L Pedersen, John M Hansen, and Jorge A.C Ambrosio, "A Roller Chain Drive Model Including Contact with Guide-Bars," Multibody System Dynamics, vol. 12, no. 3, pp. 285-301, 2004.

[39] S L Pedersen, "Model of contact between rollers and sprockets in chain-drive systems,"

Archive of Applied Mechanics, vol. 74, no. 7, pp. 489-508, 2005.

[40] Gerhard Hippmann, Martin Arnold, and Marcus Schittenhelm, "Efficient simulation of bush and roller chain drives," Multibody Dynamics, ECCOMAS Thematic Conference, June 2005.

[41] S A Metil'kov and V V Yunin, "Influence of Wear of a Roller Drive Chain on Transmission Fitness," Russian Engineering Research, vol. 28, no. 8, pp. 741-745, 2008.

[42] S A Sergeev and D V Moskalev, "Parametric Optimization of Chain-Transmission Sprockets," Russian Engineering Research, vol. 29, no. 5, pp. 452-455, 2009.

[43] Li-xin Xu, Yu-hu Yang, Zong-yu Chang, and Jian-ping Liu, "Modal analysis on transverse vibration of axially moving roller chain coupled with lumped mass," J. Cent. South Univ. Technol, vol. 18, p. 108−115, 2011.

[44] Cândida M Pereira, Jorge A Ambrósio, and Amílcar L Ramalho, "A methodology for the generation of planar models for multibody chain drives," Multibody System Dynamics, vol. 24, no. 3, pp. 303-324, 2010.

[45] Zhaowen Li and Yong Wang, "Study on the Sprocket Profile and Dynamic Analysis of Roller Chain System," vol. Computer Modeling and Simulation, 2010.

[46] www.matweb.com

[47] ASTM International , "Standard Terminology Relating to Methods of Mechanical Testing," E6-03, vol. 03.01, pp. 1-10, June 2003.